Electrolyte-Gated Organic Thin-Film Transistors

Lars Herlogsson

Norrköping 2011

Electrolyte-Gated Organic Thin-Film Transistors

Lars Herlogsson

Linköping Studies in Science and Technology. Dissertations, No. 1389
Cover: Photographs of various transistors from the papers included in this thesis

Printed by LiU-Tryck, Linköping, Sweden, 2011
ISBN 978-91-7393-088-8
ISSN 0345-7524

Abstract

There has been a remarkable progress in the development of organic electronic materials since the discovery of conducting polymers more than three decades ago. Many of these materials can be processed from solution, in the form as inks. This allows for using traditional high-volume printing techniques for manufacturing of organic electronic devices on various flexible surfaces at low cost. Many of the envisioned applications will use printed batteries, organic solar cells or electromagnetic coupling for powering. This requires that the included devices are power efficient and can operate at low voltages.

This thesis is focused on organic thin-film transistors that employ electrolytes as gate insulators. The high capacitance of the electrolyte layers allows the transistors to operate at very low voltages, at only 1 V. Polyanion-gated *p*-channel transistors and polycation-gated *n*-channel transistors are demonstrated. The mobile ions in the respective polyelectrolyte are attracted towards the gate electrode during transistor operation, while the polymer ions create a stable interface with the charged semiconductor channel. This suppresses electrochemical doping of the semiconductor bulk, which enables the transistors to fully operate in the field-effect mode. As a result, the transistors display relatively fast switching (≤ 100 µs). Interestingly, the switching speed of the transistors saturates as the channel length is reduced. This deviation from the downscaling rule is explained by that the ionic relaxation in the electrolyte limits the channel formation rather than the electronic transport in the semiconductor. Moreover, both unipolar and complementary integrated circuits based on polyelectrolyte-gated transistors are demonstrated. The complementary circuits operate at supply voltages down to 0.2 V, have a static power consumption of less than 2.5 nW per gate and display signal propagation delays down to 0.26 ms per stage. Hence, polyelectrolyte-gated circuits hold great promise for printed electronics applications driven by low-voltage and low-capacity power sources.

Populärvetenskaplig Sammanfattning

I slutet av 1970-talet fann man att det var möjligt att göra vissa typer av polymerer (plaster) elektriskt ledande. Denna upptäckt lade grunden till ett helt nytt forskningsområde, i gränslandet mellan fysik och kemi, kallat organisk elektronik. Efter många år av forskning och utveckling är det idag möjligt att tillverka en mängd olika elektroniska komponenter, som t.ex. transistorer, lysdioder och solceller, av organiska material. Ett exempel på en produkt som redan tagit sig ut på marknaden är bildskärmar baserade på organiska lysdioder (OLED). En fördel med organiska material är att de ofta kan lösas upp i lösningsmedel, vilket gör det möjligt att använda traditionella tryckmetoder för masstillverkning av elektroniska komponenter och kretsar på flexibla substrat till en mycket låg kostnad. Många av de tilltänkta produkterna kommer att använda sig av tryckta batterier eller solceller som spänningskällor. De ingående elektroniska komponenterna, t.ex. organiska transistorer, bör därför kunna drivas med låga spänningar och vara strömsnåla.

Den här avhandlingen är fokuserad på organiska tunnfilmstransistorer (TFT) i vilka det isolerande skiktet mellan *gate*-elektroden och halvledaren utgörs av en jonledande elektrolyt. Elektrolytskiktet, mellan *gate* och halvledare, erbjuder extremt hög kapacitans vilket gör det möjligt att använda väldigt låga spänningar (~1 V) för att driva denna komponent. En risk med att använda elektrolyter i organiska transistorer är att joner från elektrolyten kan tränga in i den organiska halvledaren och göra transistorn svår att styra. Detta problem har jag lyckats undvika genom att använda polyelektrolyter, material där en av jonerna representeras av en polymer. Både *p*-kanals- och *n*-kanalstransistorer kan tillverkas med polyelektrolyter som isolatormaterial. Det har gjort det möjligt att också tillverka tryckbara, snabba och strömsnåla logiska kretsar med hjälp av komplementär kretsdesign. Dessa transistorer är väl lämpade för att användas inom tryckt elektronik.

Acknowledgements

This thesis would never have become reality without the help and support from people in my surrounding, both at work and in private. I would like to express my sincere gratitude to:

Magnus Berggren, my supervisor, for giving me the opportunity to work in the Organic Electronics group, for your inspiring enthusiasm, never-ending optimism, support and encouragement.

Xavier Crispin, my co-supervisor, for arranging all the great collaborations, for your enthusiasm, encouragement and patience.

Sophie Lindesvik, for knowing just everything and all administrative help.

The entire **Organic Electronics** group, both past and present members, for your friendship, stimulating discussions, long coffee breaks, and for creating such a joyful and inspiring working environment. I would especially like to thank: **Fredrik** for leading the way to Norrköping, **Daniel** for introducing me to the Mac, **Oscar** and **Klas** for your support and the valuable scientific discussions, **Maria** and **Kristin** for your help and all good laughs.

All the **co-authors** of the included papers. Especially, I would like to thank: **Yong-Young Noh** for the great experience at Cavendish Laboratory, **Mahiar Hamedi** for all the fun scientific discussions.

All personnel at **Acreo**, especially **Bengt Råsander**, **Anurak Sawatdee** and **Mats Sandberg**, for all the help in the lab and valuable discussions.

My former colleagues at **Thin Film Electronics**, especially: **Nicklas Johansson**, for introducing me to organic electronics and transistors, **Anders Hägerström** and **Olle-Jonny Hagel**, for having all the answers to tricky processing problems.

Robert Forchheimer, for answering all my questions regarding transistor circuits.

Dennis Netzell, for your valuable advice and enormous patience in the process of finalizing this thesis.

Family and friends, for all the good times and your support.

Finally, I would like to thank my mother and father, **Ulla** and **Tryggve**, for your support and for always being there.

List of Included Papers

Paper I

Low-Voltage Polymer Field-Effect Transistors Gated via a Proton Conductor

Lars Herlogsson, Xavier Crispin, Nathaniel D. Robinson, Mats Sandberg, Olle-Jonny Hagel, Göran Gustafsson and Magnus Berggren

Advanced Materials **2007**, *19*, 97.

Contribution: All experimental work. Wrote a large part of the first draft and was involved in the final editing of the manuscript.

Paper II

Downscaling of Organic Field-Effect Transistors with a Polyelectrolyte Gate Insulator

Lars Herlogsson, Yong-Young Noh, Ni Zhao, Xavier Crispin, Henning Sirringhaus and Magnus Berggren

Advanced Materials **2008**, *20*, 4708.

Contribution: All experimental work except for the fabrication of the source and drain electrodes for sub-micrometer channels. Wrote the first draft and was involved in the final editing of the manuscript.

Paper III

Low-Voltage Ring Oscillators Based on Polyelectrolyte-Gated Polymer Thin-Film Transistors

Lars Herlogsson, Michael Cölle, Steven Tierney, Xavier Crispin and Magnus Berggren

Advanced Materials **2010**, *22*, 72.

Contribution: All experimental work. Wrote the first draft and was involved in the final editing of the manuscript.

Paper IV

Polyelectrolyte-Gated Organic Complementary Circuits Operating at Low Power and Voltage

Lars Herlogsson, Xavier Crispin, Steven Tierney and Magnus Berggren

Submitted

Contribution: All experimental work. Wrote the first draft and was involved in the final editing of the manuscript.

Paper V

Fiber-Embedded Electrolyte-Gated Field-Effect Transistors for e-Textiles

Mahair Hamedi, Lars Herlogsson, Xavier Crispin, Rebecca Morcilla, Magnus Berggren and Olle Inganäs

Advanced Materials **2009**, *21*, 573.

Contribution: Part of the experimental work. Wrote parts of the manuscript and was involved in the final editing of the manuscript.

Paper VI

A Water-Gate Organic Field-Effect Transistor

Loïg Kergoat, Lars Herlogsson, Daniele Braga, Benoit Piro, Minh-Chau Pham, Xavier Crispin, Magnus Berggren and Gilles Horowitz

Advanced Materials **2010**, *22*, 2565.

Contribution: Half the experimental work. Wrote a small part of the manuscript and was involved in the final editing of the manuscript.

Related Work Not Included in the Thesis

Polymer Field-Effect Transistor Gated via a Poly(styrenesulfonic acid) Thin Film

Elias Said, Xavier Crispin, Lars Herlogsson, Sami Elhag, Nathaniel D. Robinson and Magnus Berggren

Applied Physics Letters **2006**, *89*, 143507.

Vertical Polyelectrolyte-Gated Organic Field-Effect Transistors

Jiang Liu, Lars Herlogsson, Anurak Sawatdee, P. Favia, Mats Sandberg, Xavier Crispin, Isak Engquist and Magnus Berggren

Applied Physics Letters **2010**, *97*, 103303.

Controlling the Dimensionality of Charge Transport in Organic Thin-Film Transistor

Ari Laiho, Lars Herlogsson, Xavier Crispin and Magnus Berggren

Submitted

A Static Model for Electrolyte-Gated Organic Field-Effect Transistors

Deyu Tu, Lars Herlogsson, Loïg Kergoat, Xavier Crispin, Magnus Berggren and Robert Forchheimer

Submitted

Polyelectrolyte-Gated Organic Field-Effect Transistors

Xavier Crispin, Lars Herlogsson, Oscar Larsson, Elias Said and Magnus Berggren

Book chapter in *Iontronics – Ionic carriers in Organic Electronic Materials and Devices*, edited by J. Leger, M. Berggren and S. Carter, Taylor & Francis Group, 2011.

Transistor with Large Ion-Complexes in Electrolyte Layer

United States Patent 7646013, 2010

Table of Contents

Background

1 Introduction

1.1 From Electronics to Organic Electronics

In December 1947, John Bardeen and Walter Brattain, then scientists at Bell Laboratories in Murray Hill, New Jersey USA, constructed the first transistor. It was a germanium-based point-contact device; a kind of a bipolar junction transistor.[1] With this transistor they could build the first solid-state amplifier. Their discovery greatly intensified the research on inorganic semiconductors, which led to more discoveries and inventions, including the integrated circuit (Kilby and Noyce, 1958-59) and the metal-oxide-semiconductor field-effect transistor, or MOSFET (Atalla and Kahng, 1959). Transistors soon replaced the bulky, unreliable and power-consuming vacuum tubes, which for instance had a dramatic impact on computer design. The transistor is now the basic building block for all modern electronics and can be found in almost any electronic device, for example in computers, televisions, mobile phones and cars. The transistor has not only revolutionized the field of electronics, it has also changed the way we live our lives, in particular with respect to how we record, store and display information and how we communicate with each other. Therefore, the transistor is considered to be one of the most important inventions of the 20th century. Together with William Shockley, Bardeen and Brattain were awarded the Nobel Prize in Physics in 1956, "*for their researches on semiconductors and their discovery of the transistor effect*".

Polymers, more commonly known as plastics, have also had a strong impact on our everyday life. Due to their unique properties, relatively low cost and ease of manufacture, polymer materials have replaced many of the traditional materials, such as wood, leather, metal, glass and ceramic, in their former uses. Moreover, since the early days of Bakelite, polymers have been used as electrically insulating materials in electrical products. This has led to a widespread view of polymers as exclusively insulating materials. That was however changed in 1976, when Alan J. Heeger, Alan G. MacDiarmid and Hideki Shirakawa discovered that it was possible to change the conductivity of

the organic polymer polyacetylene by several orders of magnitude, approaching that of metals, by exposing it to iodine vapour.[2] They were awarded the Nobel Prize in Chemistry 2000 "*for the discovery and development of conductive polymers*". The conducting polymers represented a new class of materials that have the electronic and optical properties of semiconductors and metals but also with the processing advantages and mechanical properties of plastics. These findings opened the way for using organic semiconducting and conducting materials as the active material in electronic applications, and led to the creation of a new research field residing at the boundary between chemistry and physics, called *organic electronics*.

A material can be classified as being either *organic* or *inorganic*. Many centuries ago, only substances originating from living matter were regarded as organic materials and it was believed that they possessed an indefinable "living force". Today, an enormous variation of organic materials can be synthesized and organic compounds are therefore commonly just defined as any molecular material that contain the element carbon (C) in combination with other atoms.

There has been a remarkable progress in the development of organic semiconductors since the discovery of the conducting polymers more than three decades ago.[3] Many of these organic materials, especially the polymers, can be processed from solution as inks. This allows for high-volume and low-cost manufacturing of organic electronic devices on a wide range of flexible substrates, *e.g.* paper and plastic foils, by the use of traditional printing techniques, such as screen printing, gravure, offset, flexography and inkjet.[4,5] This stands in stark contrast to the very expensive and complicated methods used in traditional inorganic semiconductor device fabrication. Also, the manufacturing technology of inorganic electronics also involves the use of many hazardous materials and solvents. Another benefit with organic semiconductors is that their physical and chemical functionality can be tailored by modifying their chemical structure.[6]

A wide range of organic semiconductor devices has been developed, exemplified by the light-emitting diodes,[7] solar cells,[8,9] sensors,[10] and thin-film transistors.[11,12] Organic light-emitting diodes, or OLEDs, have attracted a lot of interest, due to the possibility to make lightweight and flexible displays and lighting products that have high brightness and that also consume low power. OLED displays are already commercial and can right now be found in many handheld products, such as mobile phones and cameras, and in the near future they will be used in large screen television screens.

1.2 The Aim and Outline of this Thesis

During the last decade, printed organic electronics has evolved to become a platform with great promise for a vast array of novel and low-cost applications within the areas of printed intelligence, large area electronics and internet-of-things.[4,13] Here, material science has proven crucial in order to improve performance of individual devices as well as of complete electronic systems, and to make electronics possible to manufacture using high-volume, roll-to-roll printing technologies. In many of the targeted applications for organic printed electronics, powering will be achieved using printed batteries,[14,15] solar cells,[9] thermoelectric generators,[16,17] or electromagnetic induction.[18] Thus, included organic components, such as transistors, should be power efficient and operate at low voltages, typically on the order of 1 V. Organic electrochemical transistors are capable of operating at such low voltages, and can also be produced by roll-to-roll printing techniques. Unfortunately, these transistors generally consume too much power and also switch slowly.[19,20] In conventional organic field-effect transistors, low-voltage operation is accomplished by using gate insulators with high capacitance. Operating voltages of merely a few volts can only be achieved by employing nanometer-thick gate insulator layers.[21,22] So thin layers are impractical to use in printed electronics applications, where robustness is one key factor. Thus, a successful development of printed electronics is today hampered by the lack of transistors and logic circuits that operates at low driving voltages and that runs at high enough speeds.

What about using an electrolyte as the gate insulator material? Electrolytes are commonly used just to achieve extraordinarily high capacitance in electrolytic capacitors. The static capacitance is virtually independent of the thickness of the electrolyte layer, which makes these materials very attractive for use in printed applications. In this thesis, electrolytes, and polyelectrolytes in particular, are explored as the gate insulator medium in organic thin-film transistors.

The idea of combining an electrolytic capacitor with a semiconductor has been exploited for instance in the so-called inorganic ion-selective field-effect transistors (ISFETs).[23] The application of a gate potential polarizes the electrolyte and leads to the formation of a thin electric double layer at the electrolyte-semiconductor interface. Importantly, due to the use of very dense inorganic materials, the ions in the electrolyte will not penetrate into the semiconductor. Therefore, this transistor operates in the field-effect mode.

This operating mode is also desired when using an electrolyte in combination with an organic semiconductor, since it ensures fast operation. However, organic semiconductors are known to be electrochemically active materials. This includes that ions penetrate the semiconductor layer and cause electrochemical doping of the semiconductor bulk. Such behaviour would seriously reduce the

operating speed of the transistor. This raises another, more fundamental question: is it possible to have a confined electric double layer at the electrolyte-organic semiconductor interface? The high capacitance of the electric double layer and the fast charging of the interface could have deep implications for printed electronics for which low-voltage operation and a moderate clock-frequency are typically required for practical circuits.

The first part of the thesis is intended to provide the necessary background information needed to understand the scientific findings in the papers, in the second part of the thesis. In the following two chapters, the physical and chemical properties of organic semiconductors and electrolytes are described. Chapter 4 gives a review of organic thin-film transistors. The typical manufacturing and characterization procedure of electrolyte-gated organic thin-film transistors are presented in chapter 5. Conclusions and a future outlook are presented in the final chapter.

2 Organic Semiconductors

2.1 Atomic Orbitals

The basic unit of matter is the atom, which consists of a dense, positively charged nucleus and a surrounding cloud of negatively charged electrons. Such microscopic systems are described by quantum mechanics, in which each elementary particle is associated with a *wave function* $\Psi(\boldsymbol{r},t)$. The square of the modulus of the wave function, $|\Psi(\boldsymbol{r},t)|^2$, is a density function that represents the probability of finding the particle at the location $\boldsymbol{r}$ at time t. The electrons of an atom can only reside in certain quantum states. Only those wave functions that are solutions of the Schrödinger equation are allowed. These wave functions are called *atomic orbitals* and they are categorized by three quantum numbers that determine the shape and energy of the orbital: the principal quantum number n that describes the energy, the orbital angular momentum quantum number l that describes the amplitude of the angular momentum, and the magnetic quantum number m_l that describes the orientation of the angular momentum. Each orbital can contain maximum two electrons, one of each spin (up or down). For historical reasons, the shells (determined by n) and the subshells (specified by l and m_l) are also labelled K, L, M, N, … and s, p, d, f, … , respectively. The two most interesting kind of atomic orbitals in organic electronics are the s orbitals, which are sphere-shaped and nonzero at the centre of the nucleus, and the p orbitals, which resemble dumbbells with their two ellipsoid-shaped lobes that are separated by a nodal plane at the nucleus (Fig. 2.1).

2.2 Molecular Orbitals and Bonds

The electrons in the outermost shell, the so-called *valence electrons*, determine the chemical, electrical and optical properties of materials. They also participate in the formation of chemical bonds with other atoms. When two atoms are brought close to one another, their atomic orbitals will start to overlap by valence electron interaction. These combined atomic orbitals form *molecular orbitals*,

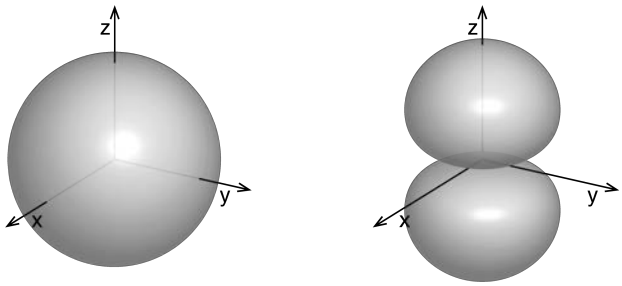

Figure 2.1 Illustrations of an *s* orbital (left) and a *p* orbital (right).

which can be represented by linear combinations of the atomic orbitals. The interactions between the atomic orbitals are either constructive (Ψ_+) or destructive (Ψ_-), leading to an increase or a decrease of the electronic density between the nuclei, respectively (Fig. 2.2). The former is a *bonding* molecular orbital and the latter an *antibonding* molecular orbital. The bonding orbital stabilizes the molecule and has lower energy than the original atomic orbitals, while the antibonding orbital destabilizes the molecule and consequently has a higher energy. Thus, there is a splitting of the original energy levels, where the separation of the energy levels indicates the strength of the atomic interactions. The electrons will fill the lower energy orbitals first, and if the total energy of the system is lower than that of the two isolated atoms, the atoms will form a stable bond. The orbital with highest energy and that is occupied with electrons is called the *Highest Occupied Molecular Orbital* (*HOMO*), and the orbital with the

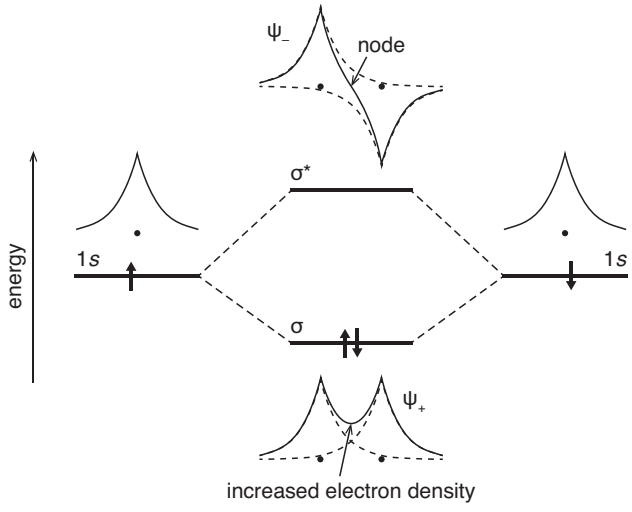

Figure 2.2 The formation of bonding and antibonding molecular orbitals and the splitting of energy levels for a dihydrogen molecule.

lowest energy that is unoccupied is called the *Lowest Occupied Molecular Orbital* (*LUMO*).

The bond is called a *σ bond* if it is symmetrical with respect to rotation about the bond axis, and a *π bond* if it is not. The orbitals in a π bond have a nodal plane passing through the nuclei. The corresponding bonds for the antibonding orbitals are called σ* and π*. The σ bonds are generally stronger than the π bonds due to the larger overlap of the atomic orbitals. Consequently, π orbitals have higher energy than σ orbitals.

The intramolecular bonds, in which the atoms share electrons, are called *covalent bonds*. The electrons in a bond may be shared unequally between the atoms, due to a difference in their electronegativity, which leads to the formation of an electric dipole moment along the bond axis. Such bonds are called *polar bonds*. A very large difference in electronegativity between the atoms involved in the bond, can lead to that the electron pair gets located almost exclusively at the more electronegative atom. Such a bond is called an *ionic bond*.

There are two types of intermolecular bonds, which both are much weaker than the intramolecular bonds. One type is the *van der Waals bond* that originates from interactions between permanent and/or induced dipoles. The second type is the *hydrogen bond*, which is an attractive interaction between hydrogen atoms and electronegative atoms carrying an electron lone pair, such as oxygen, nitrogen etc. The hydrogen bonds are stronger than the van der Waals bonds.

2.3 Hybridization

All organic materials are based on molecules that include the element carbon in combination with other atoms. The carbon atom is very versatile since it is able to form single, double and triple bonds. A carbon atom in its ground state ($1s^2\ 2s^2\ 2p_x^1\ 2p_y^1$) only has two unpaired valence shell electrons and should thus only be able to form two covalent bonds with other atoms. In order to explain the presence of methane, the virtual notion of "promotion" can be used. A carbon atom can form an excited state ($1s^2\ 2s^1\ 2p_x^1\ 2p_y^1\ 2p_z^1$) by promoting one of its 2*s* electrons to the empty 2*p* orbital so that there are four unpaired valence electrons available for bonding. The 2*s* and one, two or three of the 2*p* orbitals can be combined to form two *sp*, three sp^2 or four sp^3 *hybridized orbitals*, respectively. The respective hybrid orbitals have identical energies and shapes that resemble distorted *p* orbitals with unequal lobes, giving the orbitals a more directed orientation (see Fig. 2.3). The carbon atoms in alkanes, *e.g.* methane (CH_4), form bonds to four other atoms exclusively via single bonds. These carbons are sp^3 hybridized and their orbitals have a tetrahedral arrangement with an angle of 109.5° between them. Carbon atoms that are involved in forming a double bond,

which consists of one σ bond and one π bond, are sp^2 hybridized. These hybrid orbitals lie in one plane and are separated by an angle of 120°. The remaining unchanged $2p_z$ orbital, which is oriented perpendicular to the plane of sp^2 orbitals, participates in the double bond together with one of the sp^2 orbitals. Carbons that are *sp* hybridized form triple bonds. These hybrid orbitals point in opposite directions (180° angle) and are perpendicular to the two unchanged $2p_y$ and $2p_z$ orbitals.

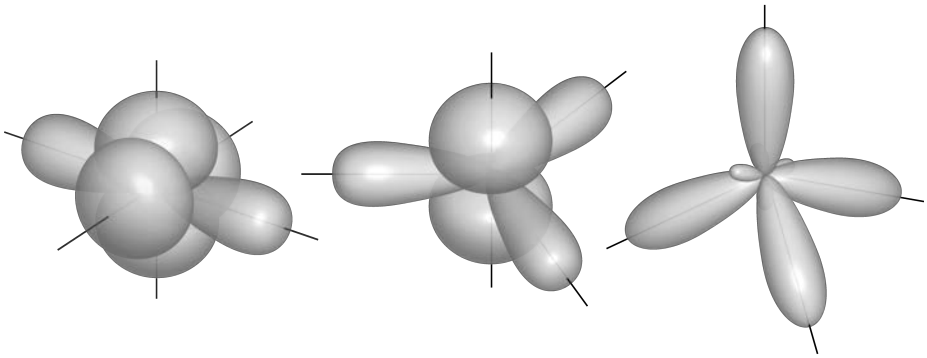

Figure 2.3 Illustrations of *sp* (left), sp^2 (centre) and sp^3 (right) hybridized orbitals.

2.4 Electronic Structure of Conjugated Materials

A conjugated molecule or polymer has a molecular framework that consists of alternating single and double carbon-carbon bonds. From a chemical structure point of view, the simplest example of a conjugated polymer is *trans*-polyacetylene, which is just composed of carbon and hydrogen atoms. All the carbon atoms are sp^2 hybridized. The sp^2 orbitals form strongly localized σ bonds, which determine the geometrical structure of the molecule. The $2p_z$ orbitals, which are oriented perpendicular to the plane of the chain, overlap and form π orbitals that extend along the conjugated chain. The electrons in these π orbitals are not associated with any specific atom or bond and are therefore *delocalized*. The number of π and π* orbitals is proportional to the number of carbon atoms in the conjugated system. Hence, there is a splitting of the energy levels as the number of carbons is doubled. This is illustrated for a series of alkenes in Figure 2.4. For an infinitely long conjugated chain, *e.g. trans*-polyacetylene, the energy difference between the energy levels becomes vanishingly small, and the energies can then be described as continuous bands rather than discrete levels. The width of the band, *W*, depends on the coupling between the atomic orbitals. Strong coupling gives wide bands. Interestingly, the HOMO and the LUMO are degenerate if the bonds in the conjugated chain are

equally long. The filled π band and the empty π* band will then coincide, resulting in a half-filled band. The polymer could thus be described as a quasi-one-dimensional metal. However, according to Peierls' theorem, such a configuration is not energetically stable. Instead, the polymer will dimerize and form alternating long single bonds (1.47 Å) and short double bonds (1.34 Å). This structural distortion, also known as the *Peierls distortion*, will stabilize the π band and destabilize the π* band, which produces a band gap, E_g, typically in the range of 1 eV to 4 eV.[24] The polymer is thus a semiconductor. The filled π band is commonly referred to as the *valence band* and the empty π* band as the *conduction band*.

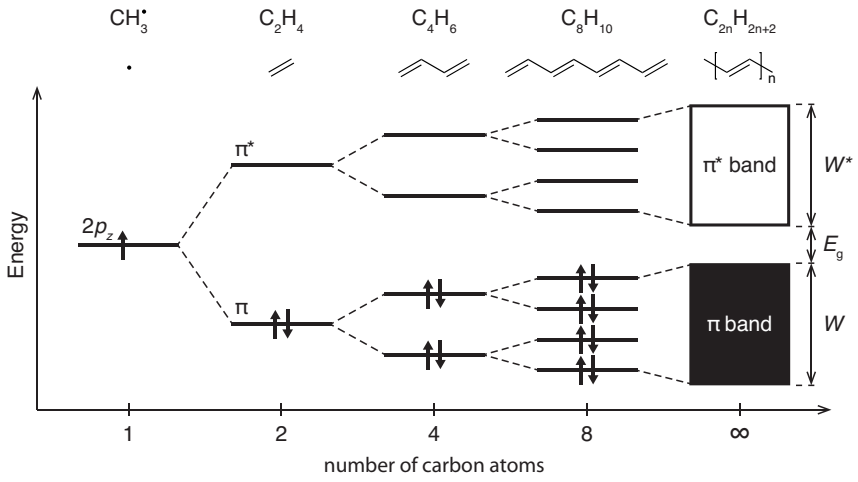

Figure 2.4 Energy level splitting and band formation in conjugated molecules.

2.5 Charge Carriers

2.5.1 Solitons

Conjugated polymers in which the two different bond length alternations give rise to equivalent structures have a degenerate ground state. One such material is *trans*-polyacetylene, which is described in Figure 2.5. The two bond length alternations, or phases, are equally likely and they can therefore be found on the same polymer chain. The boundary between the two phases is called a *soliton*. The transition between the phases is distributed over several carbon atoms, as illustrated in Figure 2.6. The bond lengths are thus equal at the centre of the soliton. The presence of a soliton will lead to the formation of a localized electronic level in the middle of the band gap. Interestingly, neutral solitons, which consist of unpaired electrons, have spin while charged solitons are

spinless. These quasiparticles are responsible for the charge transport in degenerate conjugated polymers.

2.5.2 Polarons and Bipolarons

However, most organic semiconductors have a non-degenerate ground state. For example, in polythiophenes, the aromatic form is more stable than the quinoid form (see Fig. 2.7). Solitons are therefore not encountered in these materials. The introduction of a charge into the polymer chain will be companioned by a local deformation of the surrounding bonds (see Fig. 2.8). These charge carriers, called

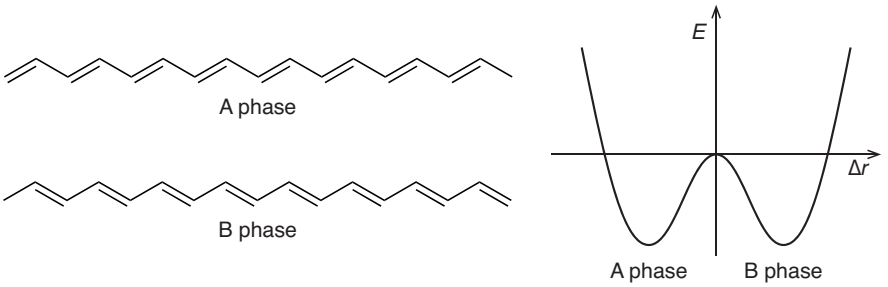

Figure 2.5 *Left*: The two structures of trans-polyacetylene with different bond length alternation, or phase. *Right*: Energy diagram illustrating the stabilization occurring due to Peierls distortion and the degenerate ground states of trans-polyacetylene.

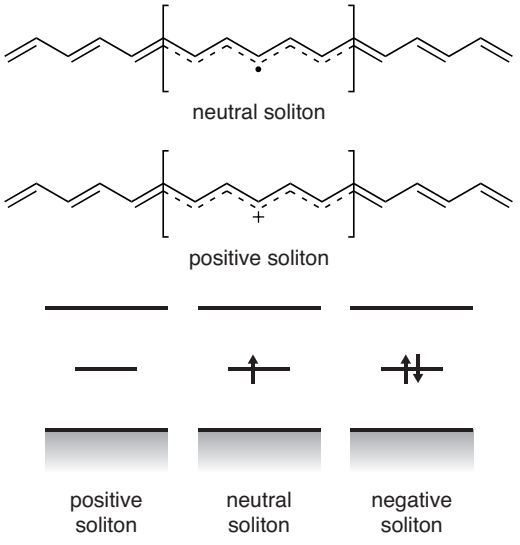

Figure 2.6 *Top*: Schematic illustrations of the geometrical structure of neutral and positively charged solitons in trans-polyacetylene. *Bottom*: Band diagrams for positively charged, neutral and negatively charged solitons.

polarons, are thus also delocalized over a few repeating units in the polymer chain. If two polarons get close to each other they can combine and form a *bipolaron*, which for some systems is more energetically stable. The band diagrams for polarons and bipolarons are shown in Figure 2.8.

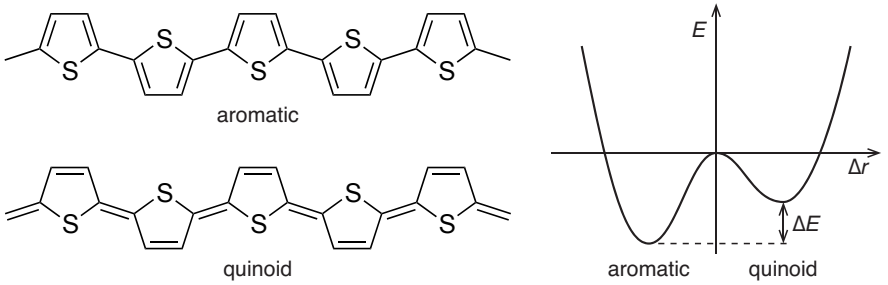

Figure 2.7 *Left*: The aromatic and quinoid forms of polythiophene. *Right*: The aromatic structure is more stable than the quinoid structure, which gives rise to a nondegenerate ground state (right).

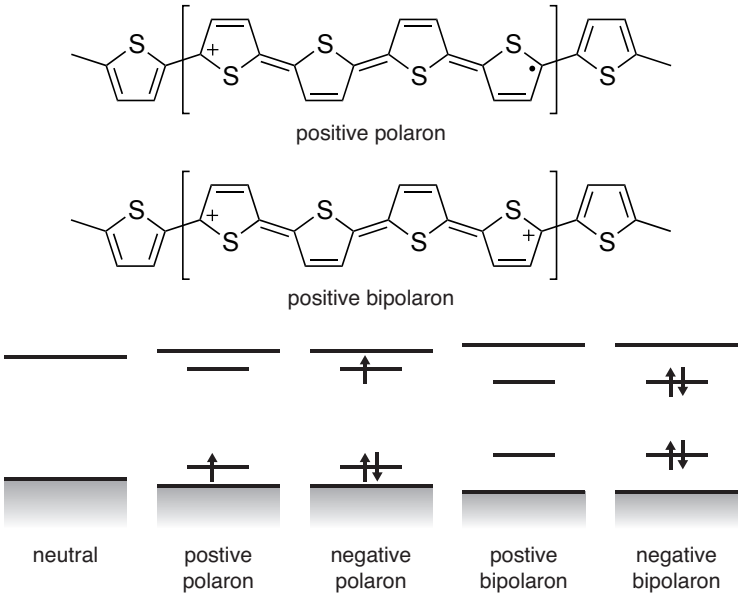

Figure 2.8 *Top*: Schematic illustrations of the geometrical structures of positively charged polarons and bipolarons in polythiophene. *Bottom*: Band diagrams for polarons and bipolarons.

2.6 Charge Transport

The charge carriers that have been described above can be efficiently transported within conjugated molecules. However, in an organic semiconductor film, the carriers need to travel over a distance that by far exceeds the size of individual conjugated molecules. The charge transport in organic materials is for that reason essentially determined by how the carriers move between neighbouring molecules.

In a perfectly ordered crystalline material, with high intermolecular π-orbital overlap, one could expect band-like transport in extended states, and consequently very high charge carrier mobility. However, due to disorder and weak van der Waals intermolecular interactions, the charge carriers in conjugated materials are typically localized to a finite number of adjacent molecules, or even to individual molecules. Thus, the charge transport in organic semiconductors is limited by trapping in localized states, which implies a thermally activated mobility.

The mobility of an organic semiconductor depends strongly on its chemical structure, purity and microstructure. Hence, conjugated materials display a wide range of charge carrier mobilities; from 10^{-6}–10^{-3} $cm^2\ V^{-1}\ s^{-1}$ in amorphous polymers, to 10–10^2 $cm^2\ V^{-1}\ s^{-1}$ in highly ordered organic single crystals.[25,26] Several different charge transport models have been developed that apply for different degrees of disorder.

Charge transport in disordered organic materials, *e.g.* amorphous and semicrystalline polymers, is generally described as thermally activated hopping in a distribution of localized states. Bässler suggested a Gaussian density of localized states to account for the spatial and energetic disorder.[27] Vissenberg and Matters used a variable-range hopping (VRH) model, where the charges can hop short distances with high activation energies or long distances with low activation energies.[28] They assumed an exponential distribution of localized states to represent the tail states of a Gaussian distribution. The VRH model predicts an increase in mobility with increasing charge carrier density. Note that in those models, the electron-phonon coupling, that is the polaron binding energy, is assumed to be negligible.

The multiple trapping and release model (MTR) has been developed to describe charge transport in well-ordered organic semiconductors, such as polycrystalline films of small molecules.[29] The MTR model assumes that transport occurs in extended states (in bands), but that most of the charge carriers are trapped in localized states, originating from impurities or defects. The trapped charges are released by thermal activation.

2.7 Doping

Pure conjugated materials are intrinsic semiconductors or insulators and usually have a rather large bandgap, typically 2–3 eV. For that reason, the number of thermally excited charge carriers is low, which make them poor conductors, typically with a charge conductivity in the range from 10^{-10} to 10^{-5} S cm^{-1}. However, the conductivity can be increased by several orders of magnitude simply by introducing more charges in the material via a doping process. Two commonly used methods are *chemical doping* and *electrochemical doping*. In both cases, the addition of electrons (*n*-doping) and the removal of electrons (*p*-doping) can chemically be seen as a reduction and an oxidation of the conjugated material, respectively.

In chemical doping, which is a redox reaction, electrons are transferred between the conjugated material (host) and the added dopants (donor or acceptor). In the case of *n*-doping, an electron is transferred from the donor dopant to the LUMO of the host. In the case of *p*-doping, an electron is transferred from the HOMO of the host to the acceptor. Polyacetylene doped with a halogen, *e.g.* chlorine, bromine, iodine etc., is a well-known example of such a material.

Electrochemical doping requires the conjugated material to be in contact with an electronically conducting working electrode and an ionically conducting electrolyte that is in contact with a counter electrode. Applying a potential difference between the two electrodes will cause an injection charges from the working electrode that are balanced by ions brought in from the electrolyte.

Both doping methods result in neutral materials where the introduced charge carriers are stabilized by the counterions from the dopant. Highly doped materials can reach metallic conductivities (1–10^4 S cm^{-1}), and are therefore often called *synthetic metals* or, in the case of polymers, (*intrinsically) conducting polymers*.

Charge carriers can also be introduced in an organic semiconductor by *photoexcitation*, as in photovoltaic devices, or by *charge injection*, as in diodes and field-effect transistors.

2.8 Organic Semiconductor Materials

There are two kinds of organic semiconductors, conjugated polymers and conjugated small molecules.

Conjugated polymers functionalized with flexible side chains are soluble and thin films can be prepared by solution-based techniques, including spin-coating, flexography, gravure and inkjet printing.[30] An example of such a material is the alkyl-substituted polythiophene poly(3-hexylthiophene) (P3HT; Fig. 2.9a).

Regioregular head-to-tail P3HT self-organize into an ordered lamellar structure with a significant overlap between the frontier π-orbitals of adjacent molecules (π-π stacking).[31] This leads to a relatively high mobility (~0.1 $cm^2 V^{-1} s^{-1}$) in the direction perpendicular to the lamellar plane.[32] Thus, the charge transport in ordered P3HT films is highly anisotropic and dependent on how the lamellae are oriented on the surface.[31] A drawback with P3HT is that it is susceptible to oxidation.[33] In response to that, thienothiophene copolymers, such as poly(2,5-bis(2-thienyl)-3,6-dihexadecylthieno[3,2-b]thiophene), ($P(T_0T_0TT_{16})$; Fig. 2.9b), have been developed that show better stability as compared to P3HT and carrier mobilities up to 1.1 $cm^2 V^{-1} s^{-1}$.[34-36]

In contrast to conjugated polymers, conjugated small-molecule materials typically have poor solubility. Hence, these materials are usually deposited by thermal sublimation in vacuum or by organic vapour phase deposition. With a control of the substrate temperature, well-organized polycrystalline films can be obtained.[29] Thus, the carrier mobility in these materials is often high. Pentacene (Fig. 2.9c), which is one of the most studied small-molecule materials, has shown mobilities as large as 6 $cm^2 V^{-1} s^{-1}$.[37]

All the materials described above are mainly hole transporting semiconductors. The observed electron mobility organic semiconductors is generally very low due to various reasons, including inefficient charge injection and more efficient trapping, *e.g.* in the presence of oxygen and water. However, several air-stable electron transporting organic semiconductors with high electron affinity (>4 eV) have been developed, and one of those is hexadecafluorocopper-phthalocyanine (F_{16}CuPc; Fig. 2.9d), which has shown an electron mobility of 0.03 $cm^2 V^{-1} s^{-1}$.[38] Recently, also conjugated polymers with high electron mobility have been synthesized, and the most promising of those is the printable material poly{[N,N'-bis(2-octyldodecyl)-naphthalene-1,4,5,8-bis(dicarbox-imide)-2,6-diyl]-alt-5,5'-(2,2'-bithiophene)} (P(NDI2OD-T2); Fig. 2.9e) with mobilities as large as 0.85 $cm^2 V^{-1} s^{-1}$.[30]

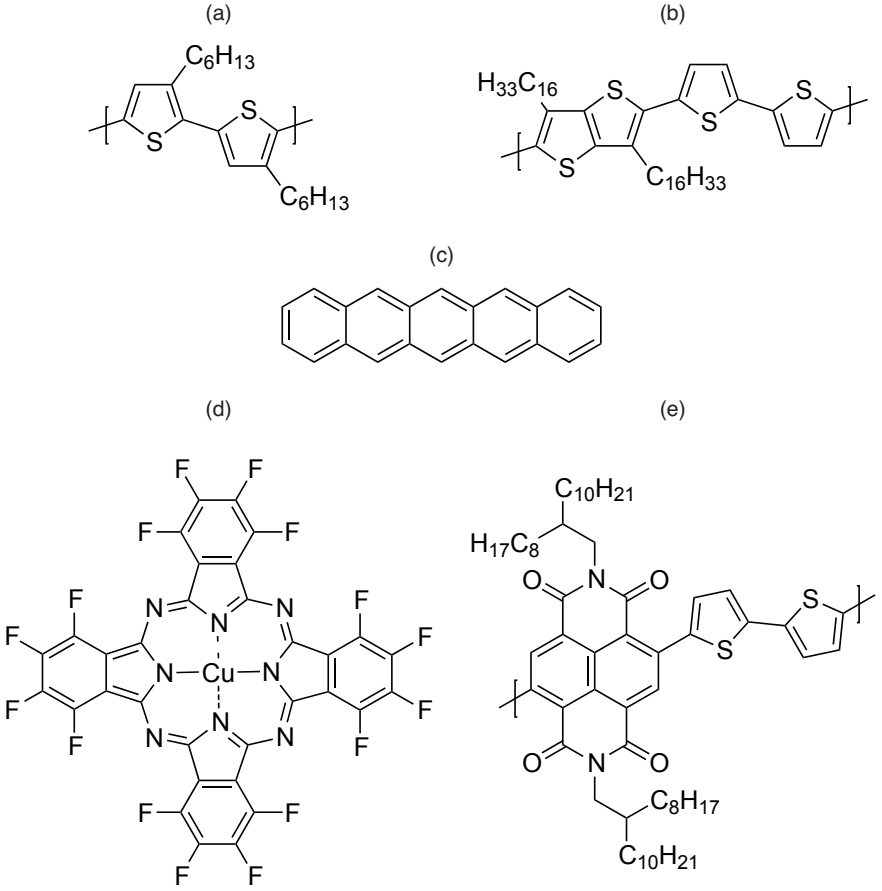

Figure 2.9 Chemical structures of some common organic semiconductors. (a) Regioregular poly(3-hexylthiophene), P3HT. (b) Poly(2,5-bis(2-thienyl)-3,6-dihexadecylthieno[3,2-b]thiophene), $P(T_0T_0TT_{16})$. (c) Pentacene. (d) Hexadecafluorocopperphthalocyanine, $F_{16}CuPc$. (e) Poly{[N,N'-bis(2-octyldodecyl)-naphthalene-1,4,5,8-bis(dicarboximide)-2,6-diyl]-alt-5,5'-(2,2'-bithiophene)}, P(NDI2OD-T2).

3 Electrolytes

Electrolytes are substances that contain free ions, which thus make them electrically conductive. Electrolytes are generally liquids, but solid and gelled forms are also common. An electrolyte consists of a salt (solute) and a solvent in which the salt dissociates to form positive ions (cations) and negative ions (anions). Moreover, electrolytes are classified as either strong or weak, depending on their degree of dissociation. Strong electrolytes are completely, or to the most part, ionized (dissociated) while weak electrolytes only are partially ionized.

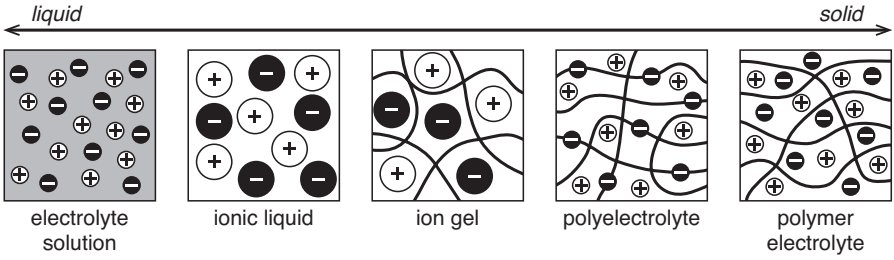

Figure 3.1 Schematic illustrations of different types of electrolytes, ordered from left to right by their physical appearance.

3.1 Types of Electrolyte Used in Organic Electronics

Different kinds of electrolytes that are of relevance for organic electronics are described below and are also schematically illustrated in Figure 3.1.

3.1.1 Electrolyte Solutions

Electrolyte solutions are the most common type of electrolytes, and they simply consist of a salt that is dissolved in a liquid medium. While dissolved, the ions will be surrounded by solvent molecules, which form a solvation shell around each ion. Water is commonly used as the dissolving medium, but other polar

non-aqueous solvents, *e.g.* alcohols, ammonia etc., can also be used. Electrolyte solutions are commonly utilized in various electrochemical applications. In such experiments, the choice of solvent may become important, since every solvent is associated with a certain safe potential window, in which it is stable. Outside this safe window, the solvent may undergo different electrochemical reactions. It is then typically better to use a non-aqueous solvent like acetonitrile, which has a relatively large safe potential window.

Pure water is actually itself an electrolyte, though a very weak one. A fraction of the water molecules will spontaneously dissociate into hydroxide ions (OH^-) and hydrogen ions (H^+). In aqueous solutions, the protons are immediately hydrated to instead form hydronium ions (H_3O^+). The concentration of ions in pure pH-neutral water is about 0.1 μM at room temperature, which gives a conductivity of 5.5×10^{-8} S cm^{-1}.

3.1.2 Ionic Liquids

An ionic liquid (IL) is simply a salt that is in the liquid state. By definition, such electrolyte systems have a melting temperature of less than 100 °C. The anions and cations are relatively large, and at least one of them usually has a delocalized charge and is organic. The physical and chemical properties of ionic liquids can be varied over a large range due to the vast selection of anions and cations. Due to its inherent liquid state, ionic liquids can exhibit high ionic conductivities, often up to 0.1 S cm^{-1}.[39] The high ionic conductivity and a wide potential window make ionic liquids attractive electrolytes for electrochemical devices. The molecular structure of an ionic liquid is given in Figure 3.2b.

3.1.3 Ion Gels

Ionic liquid are rather impractical to use in a solid-state device. However, an ionic liquid can be macroscopically immobilized by blending it with a suitable polymer, *e.g.* a block copolymer[40] or a polyelectrolyte[41] including repeat units that match the molecular structure of the ionic liquid. The resulting structure is an ion gel, which can be described as a polymer network swollen by an ionic liquid. Due to a small amount of the polymer (as little as 4 wt%), the ionic conductivity of ion gels is comparable to that of pure ionic liquids, *i.e.* in the range of 10^{-4} to 10^{-2} S cm^{-1}.[41,42]

3.1.4 Polyelectrolytes

Polyelectrolytes are polymers that have an electrolyte group in the repeat unit along the molecular backbone. These groups can dissociate when the polymer is in contact with a polar solvent, such as water, which results in a charged polymer chain and oppositely charged counterions. Polyelectrolytes that are positively charged are called polycations, while negatively charged polyelectrolytes are

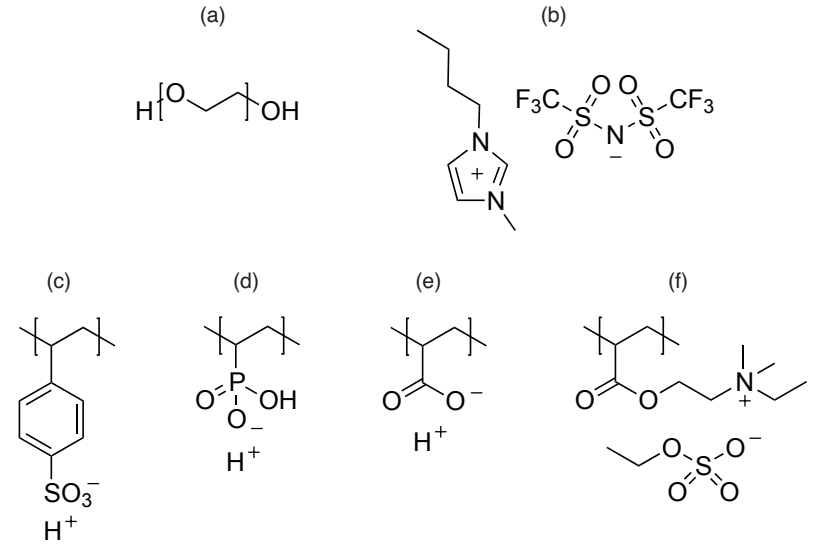

Figure 3.2 Chemical structures of various electrolytes. (a) poly(ethylene oxide), PEO. (b) 1-butyl-3-methylimidazolium bis(trifluoromethanesulfonimide), [BMIM][Tf2N]. (c) poly(styrene sulphonic acid), PSSH. (d) poly(vinyl phosphonic acid), PVPA. (e) poly(acrylic acid), PAA. (f) poly (2- ethyldimethylammonioethyl methacrylate ethyl sulfate), P(EDMAEMAES).

called polyanions. A dissociated polyelectrolyte in the solid state, *e.g.* as a thin film, will consist of mobile counterions and charged polymer chains that are effectively immobile due to their large size. Hence, solid polyelectrolytes dominantly transport ions of only one polarity, and can therefore be referred to as *n*- or *p*-type, analogous to *n*- and *p*-doped semiconductors. Actually, it is possible to build ionic transistor devices, *e.g.* bipolar junction transistors, which are analogous to conventional electronic devices.[43] The chemical structure of some polyanions and polycations are given in Figure 3.2c-f. These polyelectrolytes are hygroscopic and typically exhibit an ionic conductivity in the range from 10^{-6} to 10^{-3} S cm^{-1}.[44,45]

3.1.5 Polymer Electrolytes

A polymer electrolyte is an example of a solvent-free solid electrolyte. Polymer electrolytes are composed of a salt that is dissolved in a solvating polymer matrix. One of the most common polymer electrolytes is poly(ethylene oxide) (PEO) blended with a sodium or lithium salt. The molecular structure of PEO is shown in Figure 3.2a. Polymer electrolytes typically have an ionic conductivity in the range from 10^{-8} to 10^{-4} S cm^{-1}.[46] Polymer electrolytes have a wide range of applications and are found in various thin-film batteries, electrochromic displays, fuel cells and supercapacitors.

3.2 Ionic Charge Transport

Ions are generally transported in electrolytes by two different processes: *diffusion* and (*electro*)*migration*. In diffusion, transport of charges occurs due to a concentration gradient, while migration is the transport of charges caused by the presence of an electric field. The exact charge transport mechanisms strongly depend on the nature of the electrolyte.

Ions that move in a solvent experience a frictional force that is proportional to the viscosity of the solvent and the size of the solvated ion. The friction will limit the ionic mobility at low concentrations.

Protons are transported in a rather different manner in aqueous solutions. As described above, protons are hydrated and form hydronium ions. The hydronium ion can transfer one of its protons to a nearby water molecule, which in turn can transfer a proton to a third molecule, and so on. In other words, the protons are transported in water by a rearrangement of hydrogen bonds, a process that is known as the Grotthuss mechanism. This mechanism explains the high ionic conductivity of protons in aqueous systems. Interestingly, it has been suggested that also the protons within polyanionic systems, such as poly(vinyl phosphonic acid), are transported in a hydrogen-bonded network via a Grotthuss type mechanism.[47]

In polymer electrolytes, the ion motion is coupled to the segmental mobility of the polymer chain. The ionic conductivity will thus be low if the polymer has crystalline regions, which is problem in PEO-based electrolytes.

3.3 Electric Double Layers

The interface between a metal and an electrolyte is of interest in most electrolyte applications. A difference in electric potential between the metal electrode and the electrolyte will result in the formation of a charged interface. The electronic charge in the metal electrode will reside on the outermost surface of the electrode, while an excess of compensating and oppositely charged ions will be located in electrolyte, close to the interface. The structure of two parallel layers of positive and negative charges is called an *electric double layer* (EDL). The charge distribution in an EDL is usually described by the *Goüy-Chapman-Stern* (CGS) model, in which the electrolyte is divided into two different layers (see Fig. 3.3). The layer closest to the electrode, the *Helmholtz layer*, consists of adsorbed dipole-oriented solvent molecules and solvated ions. The Helmholtz layer and the electrode, together, can be seen as a parallel plate capacitor with a very small distance, in the order of angstroms,[48] between the two plates. The potential drop across this layer is thus linear and very steep. The next layer is called the diffuse layer and it extends relatively far into the electrolyte. It consists

of both positive and negative charges. However, compared to the bulk of the electrolyte, there is an excess of ions of opposite charge to that on the electrode and a lower concentration of ions of opposite polarity. The potential drops exponentially in this layer. The capacitance of the entire double layer is typically in the order of tens of μF cm^{-2}.[49]

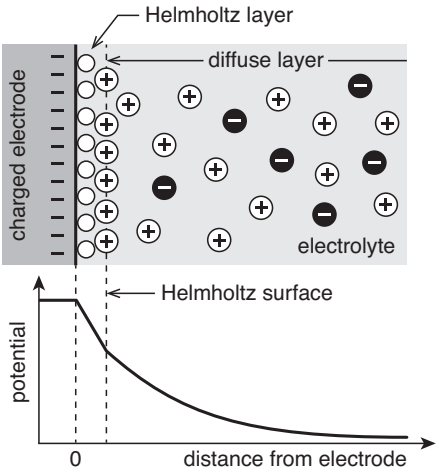

Figure 3.3 Schematic illustration of the ionic distribution in an electric double layer according to the Gouy-Chapman-Stern model. Empty circles represent solvent molecules.

3.4 Electrolytic Capacitors

Due to their ability to form electric double layers along conducting interfaces, electrolytes are attractive to use as the insulating medium in capacitors. Figure 3.4 illustrates the charging mechanism in a parallel-plate capacitor where a thin layer of electrolyte is sandwiched between two identical ion-blocking metal electrodes. The figure also illustrates the voltage profile and the electric field distribution inside the electrolyte layer. Figure 3.4b describes the situation immediately after that a voltage is applied to the capacitor. Typically, the potential drops linearly throughout the electrolyte and the induced electric field is therefore uniform within the electrolyte. The applied electric field assists alignment of the permanent and induced dipoles in the electrolyte layer (dipolar relaxation). Before any ionic relaxation takes place, the electrolyte behaves just like a dielectric medium and the induced charge density on the electrodes is proportional to the permittivity of the material. The electric field will redistribute the ions in the electrolyte layer; the anions will migrate towards the positively charged electrode while the cations will migrate towards the negatively charged

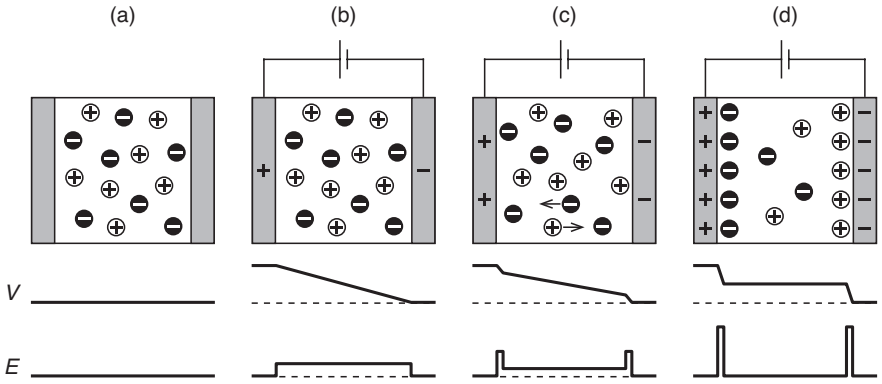

Figure 3.4 Schematic illustrations of the charge distribution, electric potential (*V*) and electric field (*E*) in the electrolyte layer of an electrolytic capacitor during charging. (a) The ions are evenly distributed when no voltage is applied. An applied voltage will induce a redistribution of the charges in the electrolyte. The situation in the electrolyte (b) before, (c) during and (d) after ionic relaxation is shown.

electrode. The electrodes get more charged as the electric double layer start to build up at the electrolyte-electrode interfaces, which leads to an increase in the potential drops right at the interfaces and the electric field within the electrolyte bulk is reduced (Fig. 3.4c). At the steady state, the electric double layers are established. Effectively, the entire applied voltage drops across the two double layers (Fig. 3.4d). Thus, the electric field becomes very high at the interfaces, but is vanishingly small in the charge-neutral electrolyte bulk.

The electrical characteristics of an electrolytic capacitor can be examined by impedance spectroscopy. The total capacitor impedance (Z) can be measured as a function of the frequency (f) of an applied alternating voltage signal. Figure 3.5 shows the measured serial capacitance and the phase angle ($\theta = \arg Z$) as a function of the frequency for an electrolytic capacitor based on a thin layer of the polycation P(VP-EDMAEMAES) (Fig. 3.2f). Based on the phase angle, the component can be classified as being either capacitive ($\theta < -45°$) or resistive ($\theta > -45°$) at a certain frequency. Three regions can be identified: a capacitive behaviour characterized by a low capacitance at high frequencies ($f > 2$ kHz), a resistive behaviour at intermediate frequencies ($25\ \text{Hz} < f < 2$ kHz), and a capacitive behaviour characterized by a high capacitance at low frequencies ($f < 25$ Hz).[45] These three regions can be associated with dipolar relaxation, ionic relaxation and the electric double layer formation, respectively, as described above.

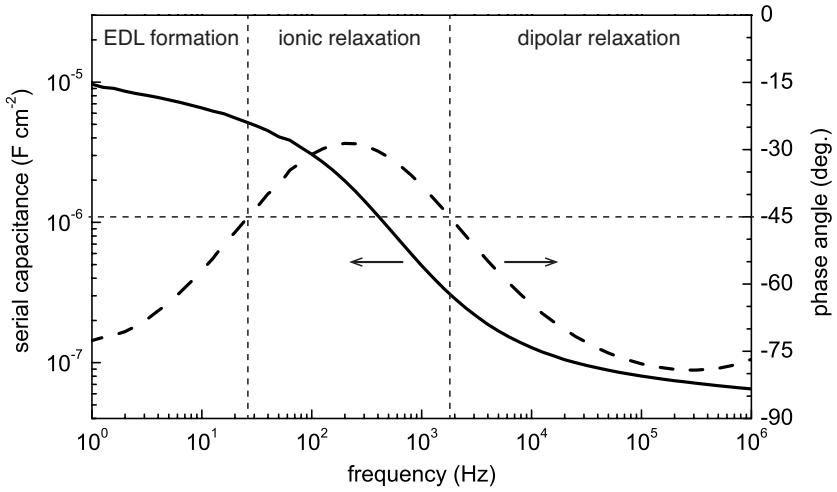

Figure 3.5 Serial capacitance (solid line) and phase angle (dashed line) *versus* the frequency of the applied voltage for a capacitor based on the polycationic electrolyte P(VP-EDMAEMAES).

An electronic device can often be represented by an equivalent electronic circuit consisting of ideal capacitors and resistors (inductors are rarely included). A simple equivalent circuit for an electrolytic capacitor is displayed in Figure 3.6.[50] In this circuit, C_E and R_E represent the dielectric capacitance and the resistance of the electrolyte, respectively. Both double layers are represented by a single capacitance C_{DL}. The impedance Z_{CT} represents a process involving any possible transfer of charges across the electrode-electrolyte interfaces. For example, this process can be an electronic leakage between the electrodes due to defects in the device or that an electrochemical reaction takes place at any of the electrode surfaces. This impedance generally only contributes to the total impedance at low frequencies (< 1 Hz) and can therefore often be ignored when the behaviour at higher frequencies are of interest.

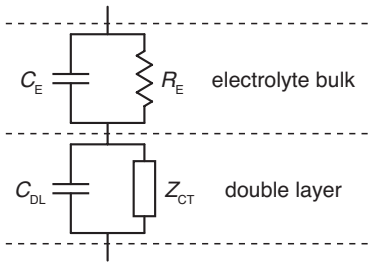

Figure 3.6 An equivalent circuit of an electrolytic capacitor.

4 Organic Thin-Film Transistors

The field-effect transistor (FET) was predicted by Julius Edgar Lilienfeld already in 1925.[51] He filed several patents describing the structure and operation of a transistor, but never succeeded in manufacturing a real functioning device. The team behind the first transistor, that is Shockley, Bardeen and Brattain, all at Bell Labs, also tried to build an FET, but they ended up in constructing a point-contact transistor instead. It would not be until 1959 that the first FET actually was demonstrated, when Dawon Kahng and Martin Atalla, scientists also from Bell Labs, manufactured a metal-oxide-semiconductor field-effect transistor (MOSFET).[52] The first MOSFETs were commercialized in 1963, and today, it is the most utilised type of transistor and it is included in nearly every electronic product. The semiconductor in these transistors is usually highly doped crystalline silicon. Besides being the active material in the transistors, it also serves as the planar substrate. Thanks to a remarkable development in miniaturization of integrated circuits, it is today possible to include billions of transistors on the same piece of substrate, or chip.

The thin-film transistor (TFT) is a special kind of field-effect transistor where the semiconductor is deposited as a thin film on an insulating substrate, such as glass or plastic foil. The semiconductors that are used in TFTs are usually intrinsic (undoped). Inorganic TFTs are commonly based on either hydrogenated amorphous silicon (a-Si:H) or polysilicon, and are extensively used in the addressing backplane for active-matrix liquid crystal displays (AMLCDs).

Practically every organic transistor that has been manufactured takes use of the thin-film transistor configuration. The first organic transistor was demonstrated in 1984 and it included an electrolyte as the gating medium.[53] It was not a field-effect effect transistor but instead an electrochemical transistor (ECT). That type of transistor has many similarities with an FET and will be further discussed in section 4.7.3. However, the first organic field-effect transistor that demonstrated clear transistor behaviour was reported by Tsumura *et al.* in 1986.[54]

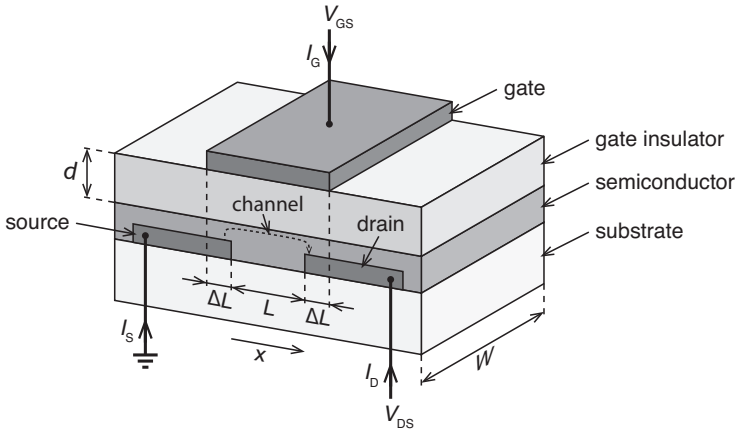

Figure 4.1 Schematic structure of a thin-film transistor with channel width *W*, channel length *L* and parasitic gate overlap Δ*L*. The dashed line indicates the charge flow in the channel.

4.1 Basic Operation

The thin-film transistor is a three-terminal device that consists of a thin semiconductor layer that is separated from a gate electrode by a layer of an electronically insulating material, which commonly is referred to as the gate insulator, or the gate dielectric if it is an electrically insulating material. This stack of materials constitutes a capacitor, which is crucial for the function of the transistor. Moreover, a source and a drain electrode are in direct contact with the semiconductor. The region between these two separated electrodes represents the channel, which has a width W and a length L given by the extensions and separation of the electrodes, respectively. A thin-film transistor is illustrated in Figure 4.1.

The source electrode is normally grounded, and it can therefore be used as the reference for the voltages applied to the gate and drain electrodes. The potential difference between the gate and the source is referred to as the gate-source voltage (V_{GS}) or just the gate voltage. Similarly, the potential difference between the drain and the source is called the drain-source voltage (V_{DS}) or simply the drain voltage. Further, the three electrode currents (I_D, I_S, I_G) are defined as positive if they flow into the device. Thus, according to Kirchhoff's current law, the sum of all three currents is zero.

As previously mentioned, the gate-insulator-semiconductor stack can be seen as a capacitor. The capacitance per unit area, C_i, of a *dielectric* gate insulator is given by

$$C_{\mathrm{i}} = \frac{\varepsilon_0 \kappa}{d} \tag{4.1}$$

where ε_0 the is the vacuum permittivity, and κ and d is the relative permittivity and the thickness of the gate insulator layer, respectively. Hence, charges can be induced at the insulator-semiconductor interface by applying a potential to the gate electrode. A positive gate voltage induces negative charges (electrons) in the semiconductor, while a negative voltage induces positive charges (holes). These charges, which are mainly confined to the first monolayer next to the insulator-semiconductor interface,[55] will dramatically increase the conductivity of the semiconductor surface so that a conducting path, a *channel*, is formed between the source and drain electrodes. A positively charged channel is called *p*-channel, and a negatively charged channel is consequently called *n*-channel. The conductance of this channel can be modulated by varying the gate voltage. Materials that can form both *p*- and *n*-channels, depending on the applied voltage, are said to be *ambipolar*.[56]

However, the applied gate voltage has to exceed a certain voltage before the channel becomes conducting. This voltage is called the threshold voltage V_{T}. In inorganic field-effect transistors that are based on doped semiconductors, *e.g.* MOSFETs, the threshold voltage corresponds to the onset of strong inversion. Organic TFTs, on the other hand, are based on intrinsic semiconductors and thus operate in the accumulation regime. The threshold voltage should therefore practically be zero. But, due to differences in the work functions of the gate material and the semiconductor, the presence of localized states (traps) at the insulator-semiconductor interface and residual charges in the bulk of the semiconductor film, the threshold voltage is generally nonzero.[57] The mobile charge Q per unit area that is induced by an applied gate voltage can therefore be written

$$Q = C_{\mathrm{i}} \left(V_{\mathrm{GS}} - V_{\mathrm{T}} \right) \tag{4.2}$$

This equation gives the charge density in the channel when the semiconductor is grounded, that is $V_{\mathrm{DS}} = 0$. But if a voltage is applied to the drain electrode, the potential V in the semiconductor will be a function of the position x in the channel. It will be a gradually increasing function, having the value 0 at the source ($x = 0$) and V_{DS} at the drain ($x = L$). Thus, the charge density is a function of the position in the channel, and is given by

$$Q(x) = C_{\mathrm{i}} \left(V_{\mathrm{GS}} - V_{\mathrm{T}} - V(x) \right) \tag{4.3}$$

Consider that a voltage larger than the threshold voltage is applied to the gate electrode. This will induce a uniform layer of charge carriers in the transistor channel (Fig. 4.2a). Applying a drain voltage will, according to Eq. (4.3), lead to a gradually decreasing charge density towards the drain electrode. It will also produce a flow of charge carriers through the channel, from the source to the drain. The resistance of the channel will effectively remain unchanged if the applied drain voltage is small ($V_{DS} \ll V_{GS} - V_T$). The drain current I_D will then be proportional to the drain voltage (Fig. 4.2a), which defines the *linear regime* of the transistor.

Increasing the drain voltage will lead to fewer induced charge carriers in the channel and consequently a higher channel resistance. This will appear as a reduced curve slope in the I_D-V_{DS} characteristics. Eventually, when $V_{DS} = V_{GS} - V_T$, the charge concentration at the drain electrode will be zero; the channel is said to "pinch off" (Fig. 4.2b). The position in the channel where the charge carrier concentration is zero is accordingly called the pinch-off point (P). Increasing the drain voltage even further ($V_{DS} > V_{GS} - V_T$) will move P, which by definition has the potential $V_{GS} - V_T$, closer to the source electrode and lead to the formation of a thin depletion region between P and the drain electrode. A space-charge limited current will flow in this depletion region. The effective channel length of the transistor, given by the distance between the source and P, will consequently be reduced to L' (Fig. 4.2c). Normally, for long-channel transistors, the reduction in channel length is negligible. That means that the number of charge carriers arriving at P will be constant when the drain voltage is increased, since both the channel length L' and the potential at P will remain unchanged. Thus, the drain current will essentially remain constant, and saturate at I_{Dsat}, when the drain voltage is higher than $V_{DSsat} = V_{GS} - V_T$. This operating region is called the *saturation regime*.

Note that positive gate and drain voltages are applied when negative charges are transported in an *n*-channel transistor, and negative voltages are applied when positive charges are transported in a *p*-channel transistor.

4.2 Transistor Equations

The current-voltage characteristics can be analytically calculated for an ideal transistor. It is assumed that the transverse electric field at the insulator-semiconductor interface that is induced by the applied gate voltage is much larger than the longitudinal electric field induced by the applied drain voltage. This is the so-called gradual channel approximation. It usually holds as long as the thickness of the gate insulator layer is much smaller than the channel length (see short-channel effects, section 4.6). It is also assumed that the mobility is constant over the entire range of different charge concentrations and electric

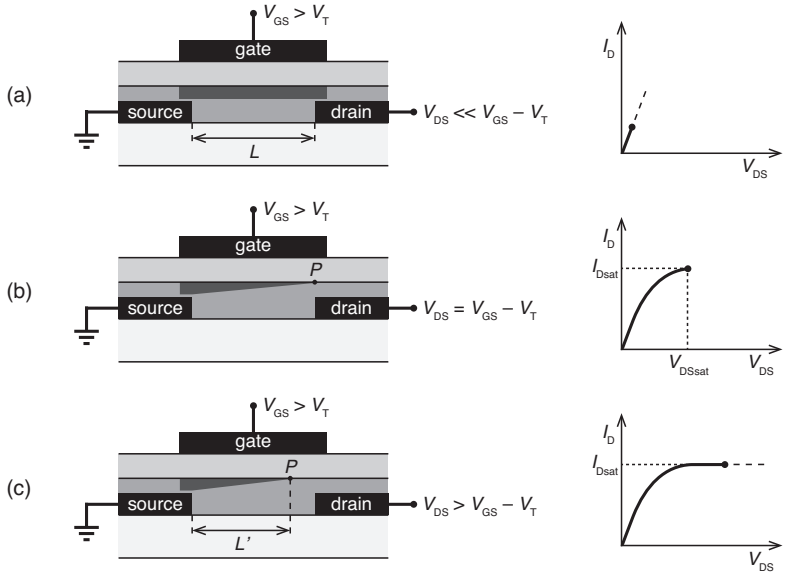

Figure 4.2 Illustrations of the charge distribution in the channel and current-voltage characteristics in the different operating regimes of field-effect transistors: (a) the linear regime; (b) the start of saturation at pinch-off; (c) the saturation regime.

fields, which is not generally true. In addition, only the drift of charges is considered. Also, the bulk of the semiconductor is assumed to have a high enough resistivity that does not contribute to the net drain current.

Since the diffusion of charge carriers is neglected, the drain current I_D at position x is given by

$$I_D(x) = W\mu Q(x) E_x(x) \tag{4.4}$$

where μ is the charge carrier mobility of the semiconductor and $E_x(x)$ is the electric field in the direction of the channel at position x. Substituting Eq. (4.3) and $E_x(x) = dV(x)/dx$ into Eq. (4.4) yields

$$I_D(x)dx = W\mu C_i \left(V_{GS} - V_T - V(x)\right) dV(x) \tag{4.5}$$

The drain current is constant along the channel. Integrating Eq. (4.5) from source to drain then gives

$$I_D = \frac{W\mu C_i}{L}\left[\left(V_{GS} - V_T\right)V_{DS} - \frac{V_{DS}^2}{2}\right] \tag{4.6}$$

In the linear regime, where $V_{DS} \ll V_{GS} - V_T$, Eq. (4.6) can be simplified to

$$I_{Dlin} = \frac{W\mu C_i}{L}\left(V_{GS} - V_T\right)V_{DS} \tag{4.7}$$

The field-effect mobility in this regime can be obtained by the derivative of Eq. (4.7)

$$\mu_{lin} = \frac{L}{WC_iV_{DS}}\frac{\partial I_D}{\partial V_{GS}} \tag{4.9}$$

The drain current at saturation is simply obtained by setting $V_{DS} = V_{GS} - V_T$ in Eq. (4.6), which yields

$$I_{Dsat} = \frac{W\mu C_i}{2L}\left(V_{GS} - V_T\right)^2 \tag{4.10}$$

The field-effect mobility in the saturation regime can be derived from Eq. (4.10)

$$\mu_{sat} = \frac{2L}{WC_i}\left(\frac{\partial\sqrt{I_{Dsat}}}{\partial V_{GS}}\right)^2 \tag{4.11}$$

The transconductance g_m is one of the most fundamental and representative transistor parameters. It describes how the drain current is modulated by the gate-source voltage, and it is defined as $g_m = \partial I_D/\partial V_{GS}$ (V_{DS} = constant). The transconductance in the linear and saturation regimes are given by

$$g_{mlin} = \frac{W\mu C_i}{L}V_{DS} \tag{4.12}$$

$$g_{msat} = \frac{W\mu C_i}{L}\left(V_{GS} - V_T\right) \tag{4.13}$$

The equations above describe the behaviour of the transistor when the gate voltage is larger than the threshold voltage. Below the threshold voltage, there is a region where the drain current depends exponentially on the gate voltage. This is the *subthreshold region*. Here, the drain current originates from diffusion, rather than drift, of charges from source to drain.[12] The slope of the drain current curve depends on the capacitance of the gate insulator and the density of interfacial traps states. The inverse slope of the logarithm of the drain current *versus* gate voltage is called the subthreshold swing S and is given by

$$S = \frac{\partial V_{GS}}{\partial\left(\log_{10} I_D\right)} \tag{4.14}$$

4.3 Current-Voltage Characteristics

Figure 4.3 shows typical current-voltage characteristics for an organic thin-film transistor. In the *output characteristics* (I_D *versus* V_{DS} for different constant V_{GS}; Fig. 4.3a), the linear regime (at low V_{DS}) and the saturation regime (at high V_{DS}) are clearly visible. The dashed curved line indicates the onset of saturation.

The *transfer characteristics* (I_D *versus* V_{GS} for constant V_{DS}) of the transistor are shown in Figure 4.3b. The drain current is usually plotted against the gate voltage in a semi-log scale since the current generally varies over several orders of magnitude. However, at low gate voltages, the drain current is very small and shows no current modulation. In this region, the drain current is limited by leakage and charging currents. This is the off-state of the transistor.

The gate voltage at which the drain current starts to increase is called the switch-on voltage (V_{SO}), or the onset voltage.[58] This is also where the subthreshold region begins. Thus, the drain current will increase exponentially with the slope $1/S$ between V_{SO} and V_T. As illustrated in the figure, the threshold voltage V_T can be estimated by taking the intersection between the gate voltage axis and the extrapolated linear fit to the square root of the drain current at saturation. However, the threshold voltage can be extracted more accurately with other techniques.[59]

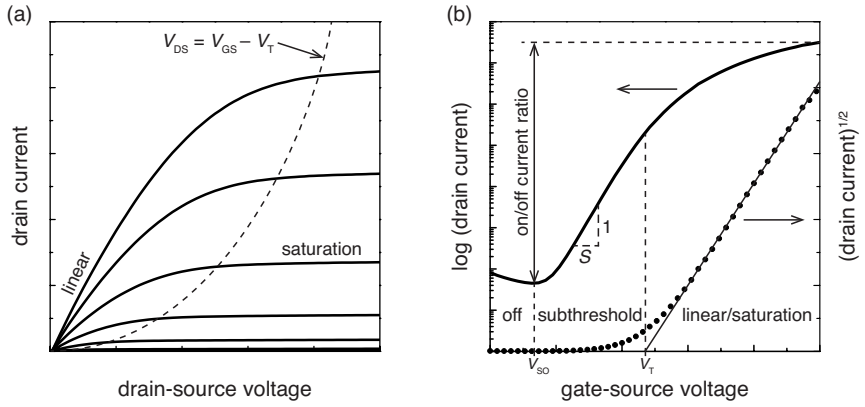

Figure 4.3 Typical current-voltage characteristics of an organic thin-film transistor. (a) Output characteristics with indications of the linear and the saturation regimes. (b) Transfer characteristics with indications of the different regimes, the on/off drain current ratio, the subthreshold swing (S), the switch-on voltage V_{SO} and the threshold voltage V_T.

Above the threshold voltage, in the on-state of the transistor, the drain current will depend on the gate and drain voltages as given by Eq. (4.6) and (4.10). The field-effect mobility in the linear and the saturation regimes can be extracted from the transfer characteristics by using Eq. (4.9) and (4.11). The ratio between the highest drain current and lowest drain current for a given drain voltage, called the on/off current ratio (I_{on}/I_{off}), can easily be determined from the transfer characteristics.

A transistor that is in the on-state at zero applied gate-source voltage is called a normally-on, or depletion mode, transistor. A transistor that is in the off-state at zero gate-source voltage is thus called a normally-off, or enhancement mode, transistor. The last kind of transistor is usually preferred in circuits for real applications.

4.4 Dynamic Performance and Cutoff Frequency

Under static conditions, when the gate and drain voltages are constant, the gate current is typically very small, and negligible compared to the drain current. However, a change in the gate-source voltage will induce a change in the charge concentration Q_G on the gate electrode. This charging will produce a gate current given by

$$I_G = \frac{\partial Q_G}{\partial t} = C_G \frac{\partial V_{GS}}{\partial t} \tag{4.15}$$

where C_G is the total gate capacitance. Applying an oscillating (sinusoidal) gate voltage will give rise to a gate current according to

$$\left|I_G\right| = 2\pi f C_G \left|V_{GS}\right| \tag{4.16}$$

Thus, the gate current increases linearly with the frequency f of the applied gate voltage. Contrariwise, the drain current is frequency independent. This means that the current gain, given by Eq. (4.17), will reduce as the frequency is increased.

$$\frac{\left|I_D\right|}{\left|I_G\right|} = \frac{g_m \left|V_{GS}\right|}{2\pi f C_G \left|V_{GS}\right|} = \frac{g_m}{2\pi f C_G} \tag{4.17}$$

The transistor is not useful when the current gain is smaller than unity. So, the frequency at which the current gain equals unity is the maximum operating frequency of a field-effect transistor. This frequency is called the *cutoff frequency*, or the transition frequency, f_T, and it is given by[12,60]

$$f_T = \frac{g_m}{2\pi C_G} \tag{4.18}$$

The gate capacitance C_G is approximately given by the sum of the channel capacitance and the parasitic gate-source and gate-drain capacitances, and can thus be written as

$$C_G \approx C_i W \left(L + 2\Delta L \right) \tag{4.19}$$

where $2\Delta L$ is the parasitic electrode overlap (see Fig. 4.1). Substituting Eq. (4.19) and the expressions for the transconductance in the linear and the saturation regimes, given by Eq. (4.12) and (4.13), into Eq. (4.18) gives

$$f_T \approx \frac{\mu V}{2\pi L\left(L + 2\Delta L \right)} \leq \frac{\mu V}{2\pi L^2} \tag{4.20}$$

where the voltage V is equal to V_{DS} in the linear regime and V_{DSsat} in the saturation regime. The two most important device parameters for the dynamic performance of transistors are thus the charge carrier mobility and the channel length. The parasitic electrode overlap ΔL can definitely have a significant impact on f_T as well, and should therefore be minimized.[60,61] Interestingly, the capacitance per unit area of the gate insulator has no influence on the cutoff frequency.

The cutoff frequency can be experimentally investigated using a ring oscillator; a circuit that is composed of an odd number of inverters connected in series in a loop (see section 4.8.4). The period of its oscillating output equals the signal delay per stage (τ) multiplied by twice the number of inverter stages. The delay time per stage is related to the cutoff frequency approximately according to $f_T \approx 1/2\tau$. Figure 4.4 present a summary of reported signal delay times as a function of supply voltages for *p*-channel,[62-68] *n*-channel,[69,70] and complementary[22,61,71-80] organic transistor circuits. The results show that there is a clear correlation between speed and supply voltage, as expected from the linear voltage dependence of f_T in Eq. (4.20). The lowest reported delay times have therefore been obtained at high supply voltages, typically at tens of volts. Most of these fast circuits are based on molecular semiconductors, which generally display relatively higher charge carrier mobility than polymeric counterparts. The graph also illustrates that rather few low-voltage circuits have been reported.

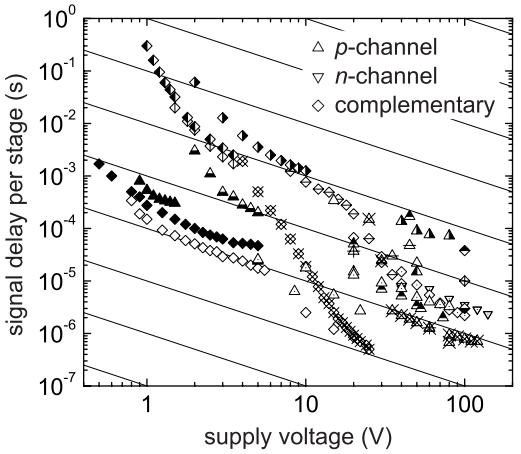

Figure 4.4 Signal delay per stage *versus* supply voltage for various reported organic thin-film transistor circuits that are based on *p*-channel, *n*-channel and complementary circuit designs. The leaning solid lines are proportional to V^{-1} and are given as help to exclude the voltage dependence of the signal delay time.

4.5 Transistor Architecture

There are basically only four different possible TFT architectures (Fig. 4.5). The stack of layers is either ordered with gate electrode positioned at the bottom (bottom-gate), or at the top (top-gate). Moreover, the source and drain electrodes are either placed underneath the semiconductor (bottom-contact), or on top it (top-contact). Each of these structures has some benefits and drawbacks. Interestingly, different TFT structures using the exact same materials can display quite dissimilar device characteristics. For example, it is of special importance how the injecting (source) contact is arranged in relation to the semiconductor and the gate electrode. In a coplanar configuration (Fig. 4.5b,d), the source and drain electrodes are situated between the insulator and the semiconductor, and as a result the charge carriers are injected directly into the channel from the edge of the electrode. In a TFT with a staggered structure (Fig. 4.5a,c), the injected charges must travel through the undoped semiconductor in order to reach the channel, but since the source and gate electrodes overlap, charges can be injected from a large area, which reduces the contact resistance.[81,82] This phenomenon is called current crowding.[83] Moreover, the work function of the source and drain electrodes should match the HOMO level in a *p*-channel transistor, and the LUMO level in an *n*-channel transistor, in order to facilitate efficient charge injection into the transistor channel. An energy barrier between the contacts and the semiconductor will give rise to a contact resistance that can affect the current-voltage characteristics of the transistor.[84] A high non-ohmic contact resistance

can often be observed in the output characteristics as superlinear current increase in the linear region.[82] The contact resistance can for instance be reduced by depositing a self-assembled monolayer on the electrode surface, which introduces a counterbalancing dipole.[59]

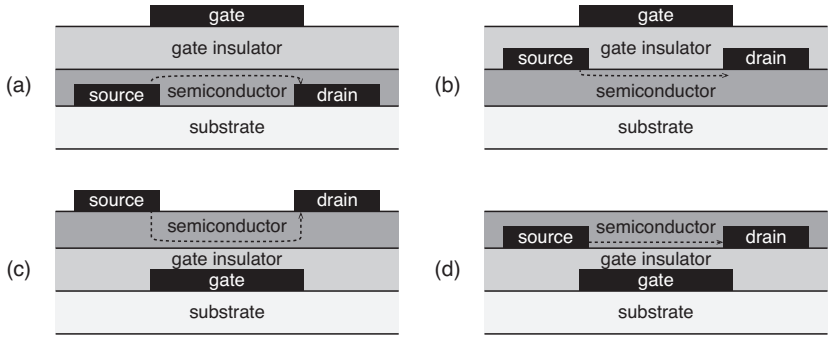

Figure 4.5 Different thin-film transistor configurations: staggered (a) top-gate/bottom-contact and (c) bottom-gate/top-contact; coplanar (b) top-gate/top-contact and (d) bottom-gate/bottom-contact. The charge flow in the channel is indicated with a dashed line.

4.6 Downscaling and Short-Channel Effects

It is generally desirable to reduce the channel length in transistors. A smaller channel length (L) will improve the performance of the transistor by increasing the transconductance ($\propto L^{-1}$) and the cutoff frequency ($\propto L^{-2}$). It will also make it possible to integrate more transistors per unit area, as the packing density is proportional to L^{-2}.

Downscaling has been the main driving force behind the tremendous progress in the performance of inorganic integrated circuits. Just as in the silicon semiconductor industry, there is a demand for fast and small integrated transistor circuits in organic electronics applications. Downscaling of organic transistors has therefore attracted great interest. Numerous techniques for accomplishing short channel lengths have been explored. Some examples on this theme are traditional photolithography,[85] electron-beam lithography,[86-88] nanoimprint lithography,[89] mask-free photolithography,[90] underetching,[91] embossing,[92] microcontact printing,[93] and self-aligned inkjet printing.[60,94-96] However, many of the reported transistors with small channel lengths have displayed deteriorated current-voltage characteristics that deviate from the ideal, long-channel behaviour, in particular with respect to drain I_D saturation.

The equations derived in section 4.2 are only valid under the constraints of the gradual channel approximation, which tells that the transversal electric field, induced by the applied gate voltage, must be much larger than the longitudinal electric field, induced by the applied drain-source voltage. That may not be fulfilled if the vertical and lateral dimensions are not equally reduced in the downscaling of the transistor. Deviations from the ideal long-channel behaviour can therefore be observed. These deviations are referred to as *short-channel effects*.[97]

The first short-channel effect that is typically observed when the channel length is reduced consists in the absence of saturation in the drain current above pinch-off. This behaviour can be explained by that the depletion region formed at the drain contact grows and eventually becomes comparable to the channel length as the drain voltage is increased. This leads to a reduction and drain voltage dependence of the effective channel length (L'). Thus, since the drain current is inversely proportional to the channel length, the drain current will increase with the drain voltage when the transistor is operated beyond pinch-off. This short-channel effect is called channel-length modulation (CLM). This effect can be accounted for, to a first approximation, by adding the term $(1 + \lambda V_{DS})$ to the equation for the drain current in the saturation regime. The constant λ is called the channel-length modulation parameter.

Some other short-channel effects can be observed in the transfer characteristics. A reduction in the channel length can lead to an increased and drain voltage dependent subthreshold current, which reduces the on/off current ratio. A drain voltage dependent shift in the threshold voltage can also be observed. This short-channel effect is called threshold voltage roll-off and is common in inorganic field-effect transistors.

If the longitudinal electric field becomes very high, the drain current may become dominated by a space-charge limited current (SCLC) flowing through the bulk of the semiconductor.[89,97] This will give the transistor diode-like output characteristics that can be described by $I_D \propto V_{DS}^n$, where $n \geq 2$.

Short-channel effects can be avoided by keeping the transverse electric field much larger than the longitudinal electric field. That is normally accomplished by reducing the thickness of the gate insulator with a least the same factor as the channel length is reduced.

4.7 Gate Insulator Materials

Charge transport in the transistor channel takes place at, or very close to, the gate insulator-semiconductor interface. Thus, the properties of the interface and the gate insulator can have a huge influence on the transistor characteristics.[98] It has

been reported that high-permittivity gate insulators can induce additional energetic disorder in the channel that enhances carrier localization and leads to a reduction of the charge carrier mobility.[99] Thus, using a low-permittivity gate insulator material can improve the performance of a transistor. It has also been shown that hydroxyl groups at the insulator interface, *e.g.* in SiO_2, create electron traps that inhibit *n*-channel conduction.[100] However, with hydroxyl-free gate insulators, such as polyethylene (PE) or benzocyclobutene derivatives (BCB), *n*-channel behaviour can in fact be observed in most organic semiconductors.

4.7.1 Low-Voltage Operation

Many of the envisioned applications for organic electronics will require transistors that are capable of operating at a low supply voltage. Low-voltage operation is accomplished by employing a gate insulator layer that has a high capacitance. Traditionally, this is done by reducing the thickness (d) of the gate insulator,[101], by employing a gate insulator material with high permittivity (κ),[102,103] or by a combination of the two approaches (see Eq. 4.1). Organic materials typically have low permittivity,[98] so it has also been common to use inorganic high-κ materials, *e.g.* oxides, as the gate insulator.[104] One of the most studied high-capacitance systems, used for TFTs with bottom-gate architecture, is the combination of a thin oxide (*e.g.* SiO_2 or AlO_x) and a self-assembled monolayer (SAM), which can provide a capacitance up to 1 $\mu F\ cm^{-2}$.[21,22,61,86,105,106] Such transistors can be operated with voltages of just a few volts.

Alternatively, instead of an electrically insulating dielectric material, an ionically conducting electrolyte can be used as the gate insulator material. This concept is far from new. The first organic transistor, demonstrated already in 1984, used a liquid electrolyte.[53] A few years later, in 1987, the same research group also made the first organic thin-film transistors including a solid-state electrolyte gate insulator.[107,108] Since then, *n*- and *p*-channel electrolyte-gated organic transistors based on a large variation of electrolyte systems, including polymer electrolytes,[109-118] polyelectrolytes,[49,119] ionic liquids,[120-124] ion gels,[42,125-132] and solutions,[133-135] have been reported. These transistors can be classified as being either field-effect transistors or electrochemical transistors, which will be further discussed in section 4.7.3.

4.7.2 Electrolytic Gate Insulators

A dielectric and an electrolytic gate insulator are compared in Figure 4.6. The figure schematically illustrates the voltage profile and the electric field distribution inside the two gate insulator materials when a negative voltage (V) is applied to the gate electrode.

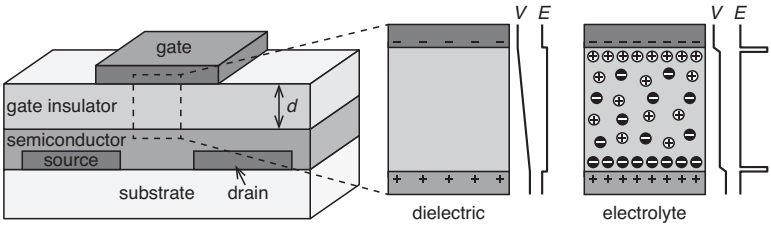

Figure 4.6 Schematic cross section of an organic thin-film transistor and illustrations of the voltage (*V*) and electric field (*E*) distributions in a dielectric and an electrolytic gate insulator when a negative gate voltage is applied.

In the case of a dielectric gate insulator, the electrostatic potential will drop linearly across the insulator layer and, consequently, it produces a constant, uniform electric field ($E = -V/d$) throughout the layer.

The static charge polarization mechanism in the electrolytic gate capacitor is essentially identical to that described for the electrolytic capacitors including two metal electrodes (see chapter 3). The only difference now is that a semiconductor represents one of the electrodes. Thus, the ions will redistribute to form EDLs at the gate-electrolyte and at the electrolyte-semiconductor interfaces, with a charge-neutral electrolyte in between them. Practically all the applied voltage will be dropped across the EDLs. The electric field will therefore be very high at the interfaces, on the order of 10^9 V m^{-1}, and negligible inside the electrolyte bulk. A high transversal electric field has been shown to suppress short-channel effects in polyelectrolyte-gated transistors with submicrometer channel lengths.[96]

The total capacitance of the electrolyte layer is determined by the capacitance of the two EDLs connected in series. Thus, the total capacitance will never be larger than the smaller of the two EDL capacitors, which usually is the EDL at the electrolyte-semiconductor interface. The capacitance is typically on the order of 10 μF cm^{-2}, which thus makes it possible to induce a very large charge carrier concentration (~10^{15} cm^{-2}) in the transistor channel at a relatively low applied gate voltages (< 3 V).[114,117] Moreover, the static capacitance of the electrolyte is virtually independent on the thickness of the layer,[136] which means that relatively thick electrolyte layers can be used to attain low-voltage operation. This is a huge advantage when it comes to manufacturing, *e.g.* using roll-to-roll production. In particular, this makes this class of transistors attractive for printed electronics applications. However, the transistor will become slower as the thickness is increased.[136]

4.7.3 Operating Modes in Electrolyte-Gated Transistors

It has been debated whether operating mechanism in electrolyte-gated transistors is electrostatic charging (field-effect) or electrochemical doping. In these transistors, the induced charges in the channel are balanced by *ions* in the electrolyte layer. In this sense, the organic semiconductor can be considered to be electrochemically doped. On the other hand, in an ideal EDL, the ionic and electronic charges are separated at the interface and compose oppositely charged sheets, in between which a uniform electric field is formed. So in this sense, the semiconductor can be considered being electrostatically charged. Thus, an electrolyte-gated transistor that forms ideal EDLs (Fig. 4.7a) can be viewed as both an electrochemical and a field-effect transistor, since it resides at the border between the two kinds. However, electrolyte-gated transistors, in which the ions are transferred across the EDL and cause electrochemical doping of the semiconductor bulk (Fig. 4.7b), are evidently not field-effect transistors. Hence, in order to distinguish between these to types of electrolyte-gated transistors, the first is referred to as an organic field-effect transistor (OFET) and the second as an organic electrochemical transistor (OECT). This notation is kept throughout the papers that are included in this thesis.

In the OECT, doping of the semiconductor produces a significant increase of the drain current since the channel becomes three-dimensional, which can be advantageous in some applications.[137,138] However, turning an OECT on and off will involve transport of ions in and out of the semiconductor bulk, which typically gives the OECT a more sluggish switching behaviour as compared to an OFET.[49] Some electrolyte-gated transistors are designed to work in the electrochemical mode,[19] while other transistors become unintentionally doped under certain circumstances. For example, a gradual transition from a field-effect mode to an electrochemical mode, as the gate voltage is increased, has been observed in transistors gated with polymer electrolytes[118,139,140] and also in transistors gated via ion gels.[127] However, employing a polyelectrolyte gate insulator can suppress parasitic bulk doping of the organic semiconductor and ensure field-effect operation.[49]

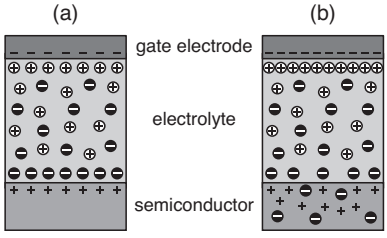

Figure 4.7 Schematic illustration of an electrolyte-gated organic thin-film transistor operating in (a) the field-effect and (b) in the electrochemical mode.

4.8 Integrated Circuits

One of the main application areas for transistors is as the signal-processing element in electronic circuits. In many senses, the most basic integrated circuit is the voltage inverter, which inverts an incoming signal V_{IN} into an outgoing signal V_{OUT}. The inverter is also a basic building block in digital electronics, where it is commonly referred to as a NOT gate. The analysis of an inverter can be used for predicting the behaviour of more complex gates such as NAND and NOR gates, which in turn are basic building blocks for more advanced circuits, such as processors.

4.8.1 Inverter Parameters

The transfer characteristics (V_{OUT} *versus* V_{IN}) for an inverter are displayed in Figure 4.8. From this graph, it is possible to extract the device parameters such as voltage amplification, or gain, noise margins and operating logic levels. The gain is defined as

$$g = \frac{\partial V_{OUT}}{\partial V_{IN}} \tag{4.21}$$

The inverter needs to have a voltage gain larger than unity in order to drive other subsequent gates. The switching threshold voltage V_M is the point in the transfer curve where the output and input voltages are equal. Ideally, this value is equal to half the applied supply voltage (V_{DD}). The parameters V_{OH} and V_{OL} are the high and low values of the output voltage, respectively. The voltage swing ($V_{OH} - V_{OL}$) of the gate should be as large as possible, ideally V_{DD}. The parameters V_{IL} and V_{IH} are defined as the operating point were $g = -1$. The noise margins for low and high inputs are given by $NM_L = V_{IL} - V_{OL}$ and $NM_H = V_{OH} - V_{IH}$, respectively. The noise margins are measures of the robustness of the inverter and should consequently be as large as possible. A high gain will normally generate large noise margins.

An inverter can be constructed with only transistors using either a unipolar or a complementary circuit design.

4.8.2 Unipolar Circuits

Unipolar circuits are composed of transistors of one and the same type, that is, the circuit only includes either *p*-channel or *n*-channel transistors. The circuit diagram for the two most common unipolar inverter designs are shown in Figure 4.9a and b. Both inverters include two enhancement-mode transistors that are connected in series. One of them represents the driver transistor and the other is the load transistor. In both designs, the input and output nodes are connected to the gate and drain contacts of the driver transistor, respectively. The gate

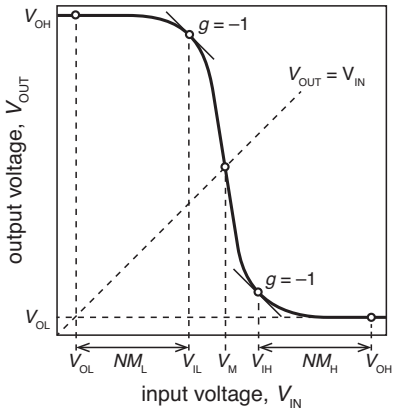

Figure 4.8 Transfer characteristics for an inverter with annotations of the most common inverter parameters.

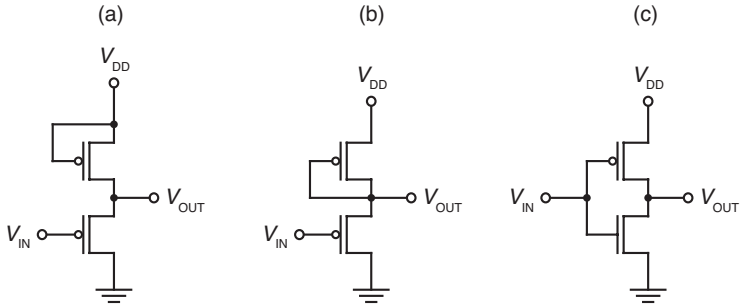

Figure 4.9 Circuit schematics of inverters with unipolar (*p*-channel) and complementary designs: (a) unipolar inverter with saturated load; (b) unipolar inverter with depleted load; (c) complementary inverter based one *p*-channel (top) and one *n*-channel (bottom) transistor.

electrode of the load transistor is either connected to its drain or to its source electrode. In the former case, the load transistor is operated in the saturation regime and the device is therefore called a *saturated load inverter* (Fig. 4.9a). In the latter case, the load transistor is always switched off. Thus, the device can be denoted to as a *depleted load inverter* (Fig. 4.9b). The load transistor in this design should preferably be a depletion-mode transistor.

Due to a more constant resistance of the load transistor, the depleted load inverter typically gives better static characteristics as compared to the saturated load inverter.[68] However, one downside with both these inverters is the high power dissipation due to the low resistance of the circuit at high input voltage.

4.8.3 Complementary Circuits

Complementary circuits includes both *n*- and *p*-channel transistors (*n*- and *p*-TFTs), both of enhancement-mode type. That means that the threshold voltages of the *n*-TFTs and the *p*-TFTs are positive and negative, respectively. That is, and $V_{Tp} < 0$ and $V_{Tn} > 0$. Complementary circuits are usually designed so that only positive voltages are used.

The circuit diagram of a complementary inverter is given in Figure 4.9c. The gate electrodes of the two TFTs are connected and serve as the input node to the inverter. The drain electrodes of the two transistors are also connected and serve as the output node. The source electrode of the *n*-TFT is connected to ground and the source electrode of the *p*-TFT is connected to the power supply (V_{DD}). The effective gate-source and drain-source voltages for the *p*-TFT are thus $V_{IN} - V_{DD}$ and $V_{OUT} - V_{DD}$, respectively.

For a low input (*e.g.* $V_{IN} = 0$), the *n*-TFT will be OFF ($V_{GSn} = 0 < V_{Tn}$) and the *p*-TFT will be ON ($|V_{GSp}| = V_{DD} > |V_{Tp}|$). The output node will then be charged to V_{DD} through the *p*-TFT.

For a high input (*e.g.* $V_{IN} = V_{DD}$), the *n*-TFT will be ON ($V_{GSn} = V_{DD} > V_{Tn}$) and the *p*-TFT will be OFF ($|V_{GSp}| = 0 < |V_{Tp}|$). The output node will then be discharged to ground through the *n*-TFT.

Note that only one of the TFTs is on in each of these two logic states. The current flow from the power supply to ground, through the transistors, will therefore be low, and limited by the off-current of the transistor that is in the off-state. A considerable current will only be conducted during the short transition period between the two logic states, when both transistors are slightly on. Thus, the static power dissipation is very low.[22] Other benefits are full rail-to-rail voltage swing, low output impedance, high gain and high noise margins. Hence, complementary circuits are essentially better than unipolar circuits in every aspect, and that is simply why this technology is so dominating today.

4.8.4 Ring Oscillators

A practical method for evaluating the dynamic performance of an integrated circuit technology, and also the included transistors, is to fabricate so-called ring oscillator circuits. A ring oscillator consists of an odd number of inverters that are connected in series, in a loop (Fig. 4.10). Due to the odd number of gates, the circuit will begin to oscillate between two voltage levels when a supply voltage is applied. In the loop, at least one of the inverters is switching its logic output state at a given time. Then, the subsequent gate will switch, and so on. The oscillation can be monitored by measuring the voltage at an output node of one of the inverters. An extra inverter can also be connected to this output node in order to prevent that the actual measurement influences the oscillation. The

period of the oscillation corresponds to the time it takes for a logic state to be changed twice of each inverter. Thus, the signal propagation delay per stage is given by

$$\tau = \frac{1}{2nf} \tag{4.22}$$

where n is the number inverters and f the frequency of the oscillation. As was pointed out in section 4.4, the signal delay is normally inversely proportional to the cutoff frequency.

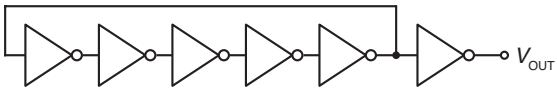

Figure 4.10 Schematic illustration of a five-stage ring oscillator with output buffer.

5 Manufacturing and Characterization of Electrolyte-Gated Transistors

The electrolyte-gated transistors that are reported in the papers included in this thesis are manufactured using different materials and methods. The ambition of this chapter is not to describe all of them, but to give a general description of how an electrolyte-gated transistor is manufactured, and also how it can be electrically characterized.

5.1 Device Fabrication

The transistor devices were fabricated in a cleanroom (class 1000-10000). All process steps were carried out in ambient atmosphere and at room temperature unless otherwise noted. All the transistors reported in the included papers have a top-gate bottom-contact configuration, but only the transistors in Paper I–IV are true thin-film transistors, since they include semiconductors, gate insulators and electrodes as thin layers on planar substrates. The general manufacturing route of such polyelectrolyte-gated organic thin-film transistors is presented below.

5.1.1 Substrate

For simplicity, the thin-film transistors are fabricated on rigid and planar surfaces. Borosilicate glass (Corning 7059 or DESAG D263) and silicon wafers with a thermally grown silicon dioxide (SiO_2) layer are therefore used as the substrates. However, it should be possible to use a flexible substrate, such as a plastic foil, as well. The substrates are carefully cleaned with solvents and then dried before further processing is performed.

5.1.2 Source and Drain Electrodes

The source and drain electrodes are patterned by traditional photolithography and wet chemical etching processing, as illustrated in Figure 5.1. First, global layers of ~5 nm chromium (as adhesion layer) and 30–60 nm gold are vacuum deposited (thermal evaporation). A uniform positive photoresist layer (0.5 μm)

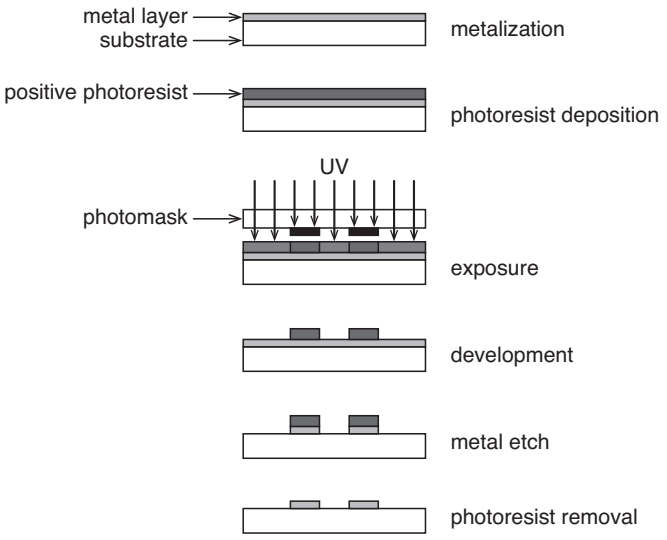

Figure 5.1 Schematic illustration of photolithographic patterning of a metal layer.

is then spin-coated on top of the metal layer and is thereafter soft-baked on a hot plate, under vacuum, in order to remove residual solvent. The photoresist layer is then exposed with UV-light through a photomask, which has the desired electrode pattern. The exposed areas of the photoresist are dissolved in a developer. The remaining photoresist will thus have the same pattern as the mask. The uncovered gold is removed by wet etching in an aqueous solution based on potassium iodide and iodine. The remaining photoresist is then removed. As a last step, the exposed parts of the thin chromium layer are removed by wet etching in a solution containing ceric ammonium nitrate, using the patterned gold electrodes as a mask.

The source and drain electrodes of the transistors in Paper I and II are relatively large (~500 µm wide) and have simple rectangular geometries that together form a single rectangular channel. The source and drain electrodes in the transistors in Paper III and IV, on the other hand, are very narrow (~3.5 µm wide) and form multiple parallel channels.

5.1.3 Organic Semiconductor Layer

The organic semiconductors (soluble conjugated polymer are here used) are dissolved in chlorinated solvents, such as chloroform or ortho-dichlorobenzene, at a concentration of 3–10 mg ml^{-1}. The solution is heated and then filtered with a hydrophobic polytetrafluoroethylene (PTFE) syringe filter with a pore size of 0.1–0.2 µm. The organic semiconductor layer is formed by spin-coating, which

typically gives a film thickness ranging from 10 to 40 nm. The film is then dried at 60 to 80 °C under dry nitrogen atmosphere, resulting in a semicrystalline film.

5.1.4 Electrolytic Gate Insulator Layer

The polyelectroytes are typically received as highly concentrated (≥ 30 wt%) water solutions. The solutions are first diluted with *n*-propanol and deionized water to give a concentration of ~10–40 mg ml^{-1}. Thus, the solvent is then a mixture of *n*-propanol and water, containing mostly *n*-propanol (75–80 %). The high concentration of the alcohol part is needed in order to make the solution wet the strongly hydrophobic semiconductor surface. Finally, the solution is filtered before it is processed using a syringe filter having a pore size of 0.1 μm. The polyelectrolyte solution is then spin-coated in nitrogen, giving a film thickness of 50–100 nm. The polyelectrolyte layers are then annealed on a hot plate under vacuum at 110 °C for 90 s.

5.1.5 Gate Electrode

Titanium gate electrodes (80–100 nm thick) are formed by thermal evaporation through a shadow mask. A simple polyimide (Kapton®) mask is used for the transistors that have simple rectangular source-drain electrodes (Paper I and II). The mask is aligned and attached to the sample manually. An electroplated nickel mask is used for the transistors that have interdigitated source-drain electrodes (Paper III and IV). The alignment of this opaque mask requires a transparent substrate, *e.g.* glass, because the sample is positioned upside-down, on top of the mask and is simply aligned by manoeuvring the sample in to place, by hand. The alignment is done with the help of a microscope, which allows for alignment accuracy better than 20 μm. Microscopy images of the two different kinds of transistors are shown in Figure 5.2.

5.1.6 Integrated Circuits

In unipolar circuits, *p*- or *n*-channel transistors are manufactured side by side. In order to make integrated circuits, all uncovered organic material around the transistors is removed by reactive-ion etching (O_2, CF_4, Ar), using the titanium gate electrodes as hard masks. Interconnects between the source, drain and gate electrodes are then formed by thermal evaporation through another shadow mask, which complete the circuits. A microscopy image of a unipolar integrated circuit is shown in Figure 5.3a.

Complementary circuits are made using the same manufacturing procedure as described above. The *p*-channel transistors are manufactured first and then dry etched to remove the exposed organic materials. Further, a fluorinated polymer is patterned on top of this first set of transistors in order to protect them from the solvents used in the subsequent process steps. The *n*-channel transistors are then

manufactured next to the first set of transistors. All exposed organic materials, including the fluorinated protective layer, are then removed using reactive-ion etching. Thereafter, interconnects are formed by vacuum deposition through a shadow mask. A microscopy image of a complementary integrated circuit is shown in Figure 5.3b.

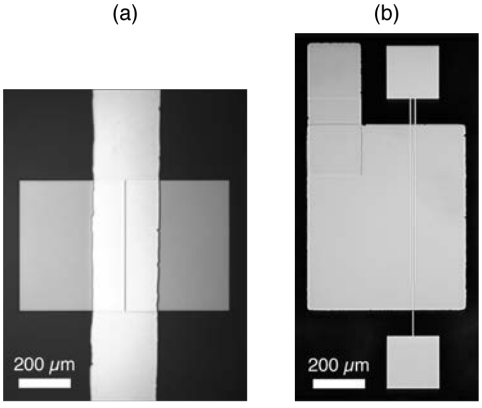

Figure 5.2 Microscope images of polyelectrolyte-gated thin-film transistors. (a) Single-channel transistor having a large parasitic electrode overlap. (b) Dual-channel transistor with interdigitated source and drain electrodes having a small parasitic electrode overlap.

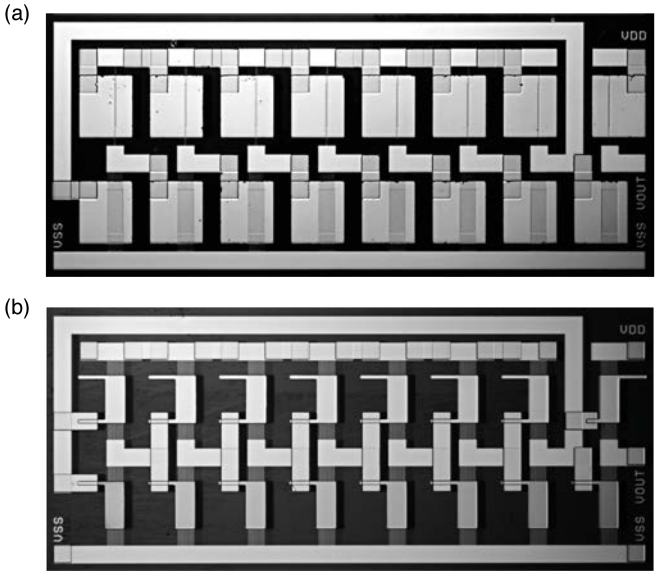

Figure 5.3 Microscope images of two integrated circuits based on polyelectrolyte-gated thin-film transistors. Seven-stage ring oscillator with output buffer with (a) unipolar design and (b) complementary design.

5.2 Electrical Characterization

In all the electrical measurements, the sample to be tested is placed on a grounded plate. Micromanipulators are used for contacting the metal electrodes on the sample, and coaxial or triaxial cables are used between the electrical characterization equipment and the micromanipulators. All measurements are carried out in air at room temperature.

5.2.1 Current-Voltage Measurement

The current-voltage characteristics of the devices, such as the output and transfer characteristics of the transistors, is measured by using a semiconductor parameter analyzer that is equipped with several source-measurement units (SMUs). Each SMU can supply a constant current or a constant voltage and, at the same time, measure the current and the voltage. For standard electrical characterisation, each terminal of the device is connected to an SMU.

The output characteristics (see Fig. 4.3a) are measured as follows: The drain current is measured as the drain voltage is swept, or actually changed in small steps, from a starting value (0 V) to an end value, while the gate voltage is kept constant. This is repeated for a number of, normally equally spaced, gate voltages.

The transfer characteristics (see Fig. 4.3b.) are measured in similar manner. The drain current is measured while the gate voltage is swept and the drain voltage is held constant. The gate voltage is swept over a range that extends from the off-state to the on-state. This measurement is normally performed for a small and a large drain voltage in order to record the drain current in the linear regime and the saturation regime.

In both measurements, the sweeping parameter is often swept from the starting value, to the end value, and then back again to the starting value (a dual sweep). This is done in order to investigate if any hysteresis can be found in the *I-V* characteristics.

5.2.2 Transient Measurements

The switching characteristics of the transistors were measured by using the setup displayed in Figure 5.4a. In this measurement, the voltage drop V_S over a resistor inserted between the source contact and ground is recorded with an oscilloscope, while the potential at the drain contact is held at a constant potential V_D with a DC power supply and a square voltage pulse V_G is applied to the gate electrode with an arbitrary waveform generator. The source current I_S then equals

$$I_S = \frac{V_S}{R} \tag{5.1}$$

The value of the resistance R is selected so that only a fraction of the applied drain voltage is dropped over the resistor, *i.e.* $|V_S| \ll |V_D|$.

The recorded source current is the sum of two contributions: an exponentially decaying current originating from the charging of the gate capacitor, *i.e.* the charging current, and the current that flows between the source and the drain contact, *i.e.* the transistor channel current. The charging current dominates the recorded current immediately after that the gate voltage has been changed or applied. Thus, the initial build-up (or disruption) of the transistor channel is not measureable. However, if the drain contact is grounded, the recorded source current will only consist of the charging current component, since the channel current evidently is zero. Thus, the channel current can be extracted by taking the difference between the source currents recorded for $V_D \neq 0$ and $V_D = 0$, as illustrated in Figure 5.4b.

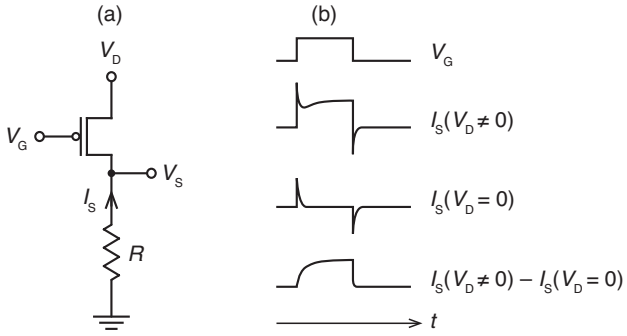

Figure 5.4 (a) Circuit schematic of the measurement setup used in the transient measurements. (b) Illustration of how the channel current can be extracted from the transient curves.

5.2.3 Impedance Spectroscopy

Impedance spectroscopy is a powerful technique to characterize the electrical properties of various materials including those of electrolytes. The material to be tested is sandwiched between two electrodes, thus forming a capacitor. The impedance of the sample is measured by applying an alternating voltage with a fixed frequency f to the capacitor. This will generate an alternating current of the same frequency. There will generally be a phase shift between the current and voltage signals, which can be described by the phase angle θ. The amplitude and the phase shift of the current signal are measured for a number of frequencies in a given range, usually going from high to low frequencies. This allows for expressing the impedance as function of frequency. The frequency-dependent complex impedance of the sample is given by

$$Z^* = \frac{U^*}{I^*} \tag{5.2}$$

where U^* is the complex applied voltage and I^* is the complex measured current. The complex impedance can be expressed as a sum of a real and an imaginary impedance as

$$Z^* = Z_{\mathrm{Re}} + iZ_{\mathrm{Im}} \tag{5.3}$$

The phase angle can then be written as

$$\theta = \tan^{-1}\left(\frac{Z_{\mathrm{Im}}}{Z_{\mathrm{Re}}}\right) \tag{5.4}$$

In order to calculate the *effective* capacitance of the sample, an equivalent circuit has to be chosen that reflects the behaviour of the sample. The equivalent circuit either consists of a capacitor *in series* or *in parallel* with a resistor. The capacitance for the first alternative is called the serial capacitance C_s while the other is called the parallel capacitance C_p, and they can be calculated according to

$$C_s = -\frac{1}{2\pi f Z_{\mathrm{Im}}} \tag{5.5}$$

$$C_p = -\frac{1}{2\pi f Z_{\mathrm{Im}}\left[1+\left(Z_{\mathrm{Re}} / Z_{\mathrm{Im}}\right)^2\right]} \tag{5.6}$$

6 Conclusions and Future Outlook

This thesis is entirely focused on organic thin-film transistors that employ electrolytes as the gate insulator. The application of a gate bias will polarize the electrolyte. Ions in the electrolyte will accumulate at the semiconductor interface and form a so-called electric double layer (EDL) together with oppositely charged electronic charge carriers in the organic semiconductor layer, which have been injected from the source contact. The very small distance (in the order of angstroms) between the two charged layers results in a very high capacitance, typically in the order of tens of μF cm^{-2}, which allows the transistors to operate at low voltage, around 1 V. Interestingly, the capacitance is virtually independent on the thickness of the electrolyte layer. This is advantageous when it comes to manufacturing of the transistors. It also means that the position of the gate electrode becomes less critical, which opens up for alternative transistor designs. For example, an electrolyte-gated transistor could be formed at the junction between two microfibers (Paper V), or the transistor could be gated via a droplet of pure water (Paper VI).

A question was raised in the introduction, whether it is possible to have a confined EDL at the electrolyte-semiconductor interface or not. To address this issue, we have used polyelectrolytes as the gate insulator material (Paper I–IV). Polyelectrolytes are polymers that consist of charged polymer chains and mobile counterions. Thus, polyelectrolytes dominantly transport ions of only one polarity, and can therefore be referred to as either *n*- or *p*-type, analogous to *n*- and *p*-doped semiconductors. In the reported transistors, the polyelectrolyte is matched with the organic semiconductor such that the mobile ions are depleted from the electrolyte-semiconductor interface when the transistor is operated in the accumulation mode. In other words, *p*-type polyanions are used in *p*-channel transistors and *n*-type polycations are used in *n*-channel transistors. Consequently, during transistor operation, the EDL at this interface will be composed of polyions in the gate insulator and electronic charges in the semiconductor. The polyions are, due to their size, virtually immobile and cannot penetrate into the semiconductor. Hence, these material combinations suppress

electrochemical doping of the semiconductor bulk, which implies that just interfacial charging takes place. This statement is supported by that the observed current levels are moderate, that very little hysteresis are observed in the current-voltage characteristics and that the transistors display relatively fast switching (≤ 100 µs).

A special feature of these transistors is that the switching speed saturates as the channel length is reduced. This deviation from the downscaling rule is explained by that the ionic relaxation in the electrolyte will limit the channel formation rather than the electronic transport in the semiconductor. However, a benefit with using an electrolyte as the gate insulator in transistors with small channel lengths is that the high electric field in the EDL suppresses short-channel effects (Paper II).

The use of solid electrolytes makes it possible to manufacture integrated circuits. Unipolar circuits based on polyanion-gated *p*-channel transistors that operated at voltages down to 0.9 V and display signal propagation delays down 0.3 ms per stage have been made (Paper III). The successful demonstration of both *p*- and *n*-channel polyelectrolyte-gated transistors also allows for making low-voltage complementary integrated circuits. Such demonstrated circuits operate at supply voltages down to 0.2 V, have a static power consumption of less than 2.5 nW per logic gate and display signal propagation delays down to 0.26 ms per stage (Paper IV).

The low operating voltage, relatively fast operating speed and low power consumption make these polyelectrolyte-gated organic thin-film transistors a promising candidate for use in printed electronics applications. However, there are still a few hurdles to overcome before that can become reality. For example, there are challenges with printing hydrophilic polyelectrolytes on strongly hydrophobic semiconductor surfaces, or vice versa. This may require the use of adhesion promoting layers or the use of specially synthesized polyelectrolyte and organic semiconductor materials. Another challenge is to accomplish short channel lengths with printed source and drain electrodes. Hence, in order to obtain acceptable circuit speeds, high-mobility semiconductors have to be employed. Moreover, the operating speed of the demonstrated transistors is limited by the polarization of the polyelectrolytes. Increasing the ionic conductivity of these layers should make these transistor circuits even faster.

References

[1] J. Bardeen, W. H. Brattain, *Physical Review* **1948**, *74*, 230.

[2] H. Shirakawa, E. J. Louis, A. G. MacDiarmid, C. K. Chiang, A. J. Heeger, *J. Chem. Soc., Chem. Commun.* **1977**, 578.

[3] A. J. Heeger, *Chem. Soc. Rev.* **2010**, *39*, 2354.

[4] A. C. Arias, J. D. MacKenzie, I. McCulloch, J. Rivnay, A. Salleo, *Chem. Rev.* **2010**, *110*, 3.

[5] D. Tobjörk, R. Österbacka, *Adv. Mater.* **2011**, *23*, 1935.

[6] J. E. Anthony, A. Facchetti, M. Heeney, S. R. Marder, X. Zhan, *Adv. Mater.* **2010**, *22*, 3876.

[7] J. H. Burroughes, D. D. C. Bradley, A. R. Brown, R. N. Marks, K. Mackay, R. H. Friend, P. L. Burns, A. B. Holmes, *Nature* **1990**, *347*, 539.

[8] T. Ameri, G. Dennler, C. Lungenschmied, C. J. Brabec, *Energy Environ. Sci.* **2009**, *2*, 347.

[9] C. N. Hoth, P. Schilinsky, S. A. Choulis, C. J. Brabec, *Nano Letters* **2008**, *8*, 2806.

[10] D. A. Bernards, R. M. Owens, G. G. Malliaras, *Organic Semiconductors in Sensor Applications*, Springer, New York **2008**.

[11] H. Sirringhaus, *Adv. Mater.* **2005**, *17*, 2411.

[12] H. Klauk, *Chem. Soc. Rev.* **2010**, *39*, 2643.

[13] L. W. F. Chaves, C. Decker, "A survey on organic smart labels for the Internet-of-Things", presented at *7th International Conference on Networked Sensing Systems (INSS), 2010*, Kassel, Germany, **2010**.

[14] I. Ferreira, B. Br·s, J. I. c. Martins, N. Correia, P. Barquinha, E. Fortunato, R. Martins, *Electrochim. Acta* **2011**, *56*, 1099.

[15] M. Hilder, B. Winther-Jensen, N. B. Clark, *J. Power Sources* **2009**, *194*, 1135.

[16] O. Bubnova, Z. U. Khan, A. Malti, S. Braun, M. Fahlman, M. Berggren, X. Crispin, *Nat Mater* **2011**, *10*, 429.

[17] Y. Xuan, X. Liu, S. Desbief, Lecl, egrave, P. re, M. Fahlman, R. Lazzaroni, M. Berggren, J. Cornil, D. Emin, X. Crispin, *Phys. Rev. B* **2010**, *82*, 115454.

[18] M. Bohm, A. Ullmann, D. Zipperer, A. Knobloch, W. H. Glauert, W. Fix, "Printable electronics for polymer RFID applications", San Francisco, CA, United states, **2006**.

[19] D. Nilsson, M. Chen, T. Kugler, T. Remonen, M. Armgarth, M. Berggren, *Adv. Mater.* **2002**, *14*, 51.

[20] D. Nilsson, N. Robinson, M. Berggren, R. Forchheimer, *Adv. Mater.* **2005**, *17*, 353.

[21] H. Klauk, U. Zschieschang, M. Halik, *J. Appl. Phys.* **2007**, *102*, 074514.

[22] H. Klauk, U. Zschieschang, J. Pflaum, M. Halik, *Nature* **2007**, *445*, 745.

[23] P. Bergveld, *Sens. Actuators B* **2003**, *88*, 1.

[24] G. Tzamalis, V. Lemaur, F. Karlsson, P. O. Holtz, M. Andersson, X. Crispin, J. Cornil, M. Berggren, *Chem. Phys. Lett.* **2010**, *489*, 92.

[25] O. D. Jurchescu, J. Baas, T. T. M. Palstra, *Appl. Phys. Lett.* **2004**, *84*, 3061.

[26] W. Warta, N. Karl, *Phys. Rev. B* **1985**, *32*, 1172.

[27] H. Bässler, *Phys. Status Solidi A* **1993**, *175*, 15.

[28] M. C. J. M. Vissenberg, M. Matters, *Phys. Rev. B: Condens. Matter Mater. Phys.* **1998**, *57*, 12964.

[29] G. Horowitz, R. Hajlaoui, P. Delannoy, *J. Phys. III* **1995**, *5*, 355.

[30] H. Yan, Z. Chen, Y. Zheng, C. Newman, J. R. Quinn, F. Dotz, M. Kastler, A. Facchetti, *Nature* **2009**, *457*, 679.

[31] H. Sirringhaus, P. J. Brown, R. H. Friend, M. M. Nielsen, K. Bechgaard, B. M. W. Langeveld-Voss, A. J. H. Spiering, R. A. J. Janssen, E. W. Meijer, P. Herwig, D. M. de Leeuw, *Nature* **1999**, *401*, 685.

[32] H. Sirringhaus, N. Tessler, R. H. Friend, *Science* **1998**, *280*, 1741.

[33] M. S. A. Abdou, F. P. Orfino, Y. Son, S. Holdcroft, *J. Am. Chem. Soc.* **1997**, *119*, 4518.

[34] I. McCulloch, M. Heeney, M. L. Chabinyc, D. DeLongchamp, R. J. Kline, M. Cölle, W. Duffy, D. Fischer, D. Gundlach, B. Hamadani, R. Hamilton, L. Richter, A. Salleo, M. Shkunov, D. Sparrowe, S. Tierney, W. Zhang, *Adv. Mater.* **2009**, *21*, 1091.

[35] I. McCulloch, M. Heeney, C. Bailey, K. Genevicius, I. MacDonald, M. Shkunov, D. Sparrowe, S. Tierney, R. Wagner, W. Zhang, M. L. Chabinyc, R. J. Kline, M. D. McGehee, M. F. Toney, *Nature Mater.* **2006**, *5*, 328.

[36] H. Ohkita, S. Cook, Y. Astuti, W. Duffy, S. Tierney, W. Zhang, M. Heeney, I. McCulloch, J. Nelson, D. D. C. Bradley, J. R. Durrant, *J. Am. Chem. Soc.* **2008**, *130*, 3030.

[37] H. S. Tan, N. Mathews, T. Cahyadi, F. R. Zhu, S. G. Mhaisalkar, *Appl. Phys. Lett.* **2009**, *94*, 263303.

[38] Z. Bao, A. J. Lovinger, J. Brown, *J. Am. Chem. Soc.* **1998**, *120*, 207.

[39] R. Hagiwara, K. Matsumoto, Y. Nakamori, T. Tsuda, Y. Ito, H. Matsumoto, K. Momota, *J. Electrochem. Soc.* **2003**, *150*, D195.

[40] Y. He, P. G. Boswell, P. Buhlmann, T. P. Lodge, *J. Phys. Chem. B* **2007**, *111*, 4645.

[41] R. Marcilla, F. Alcaide, H. Sardon, J. A. Pomposo, C. Pozo-Gonzalo, D. Mecerreyes, *Electrochem. Commun.* **2006**, *8*, 482.

[42] J. H. Cho, J. Lee, Y. He, B. Kim, T. P. Lodge, C. D. Frisbie, *Adv. Mater.* **2008**, *20*, 686.

[43] K. Tybrandt, K. C. Larsson, A. Richter-Dahlfors, M. Berggren, *Proc. Natl. Acad. Sci. U. S. A.* **2010**, *107*, 9929.

[44] A. Kaltbeitzel, S. Schauff, H. Steininger, B. Bingol, G. Brunklaus, W. H. Meyer, H. W. Spiess, *Solid State Ionics* **2007**, *178*, 469.

[45] O. Larsson, E. Said, M. Berggren, X. Crispin, *Adv. Funct. Mater.* **2009**, *19*, 3334.

[46] A. M. Stephan, *Eur. Polym. J.* **2006**, *42*, 21.

[47] Y. J. Lee, B. Bingol, T. Murakhtina, D. Sebastiani, W. H. Meyer, G. Wegner, H. W. Spiess, *J. Phys. Chem. B* **2007**, *111*, 9711.

[48] D. C. Grahame, *Chem. Rev.* **1947**, *41*, 441.

[49] L. Herlogsson, X. Crispin, N. D. Robinson, M. Sandberg, O.-J. Hagel, G. Gustafsson, M. Berggren, *Adv. Mater.* **2007**, *19*, 97.

[50] H. Yuan, H. Shimotani, J. Ye, S. Yoon, H. Aliah, A. Tsukazaki, M. Kawasaki, Y. Iwasa, *J. Am. Chem. Soc.* **2010**, *132*, 18402.

[51] J. E. Lilienfeld, *United States Patent 1745175*, Method and apparatus for controlling electric currents, **1930**.

[52] D. Kahng, *United States Patent 3102230*, Electric field controlled semiconductor device, **1963**.

[53] H. S. White, G. P. Kittlesen, M. S. Wrighton, *J. Am. Chem. Soc.* **1984**, *106*, 5375.

[54] A. Tsumura, H. Koezuka, T. Ando, *Appl. Phys. Lett.* **1986**, *49*, 1210.

[55] G. Horowitz, *Synth. Met.* **2003**, *138*, 101.

[56] J. Zaumseil, H. Sirringhaus, *Chem. Rev.* **2007**, *107*, 1296.

[57] G. Horowitz, in *Semiconducting Polymers*, Vol. 2 (Eds: G. Hadziioannou, G. C. Malliaras), Wiley-VCH Verlag GmbH & Co. KGaA, Weinheim, Germany **2007**.

[58] E. J. Meijer, C. Tanase, P. W. M. Blom, V. E. Van, B. H. Huisman, L. D. M. De, T. M. Klapwijk, *Appl. Phys. Lett.* **2002**, *80*, 3838.

[59] D. Boudinet, G. Le Blevennec, C. Serbutoviez, J.-M. Verilhac, H. Yan, G. Horowitz, *J. Appl. Phys.* **2009**, *105*, 084510.

[60] Y.-Y. Noh, N. Zhao, M. Caironi, H. Sirringhaus, *Nature Nanotech.* **2007**, *2*, 784.

[61] F. Ante, F. Letzkus, J. Butschke, U. Zschieschang, K. Kern, J. N. Burghartz, H. Klauk, "Submicron Low-Voltage Organic Transistors and Circuits Enabled by High-Resolution Silicon Stencil Masks", presented at *International Electron Devices Meeting (IEDM), 2010*, Piscataway, NJ, USA, **2010**.

[62] A. R. Brown, C. P. Jarrett, D. M. de Leeuw, M. Matters, *Synth. Met.* **1997**, *88*, 37.

[63] S. De Vusser, S. Steudel, K. Myny, J. Genoe, P. Heremans, "High-performance low voltage organic thin-film transistors", Warrendale, PA 15086, United States, **2005**.

[64] F. Eder, H. Klauk, M. Halik, U. Zschieschang, G. Schmid, C. Dehm, *Appl. Phys. Lett.* **2004**, *84*, 2673.

[65] J. Ficker, A. Ullmann, W. Fix, H. Rost, W. Clemens, *J. Appl. Phys.* **2003**, *94*, 2638.

[66] W. Fix, A. Ullmann, J. Ficker, W. Clemens, *Appl. Phys. Lett.* **2002**, *81*, 1735.

[67] S. H. Han, S. M. Cho, J. H. Kim, J. W. Choi, J. Jang, M. H. Oh, *Appl. Phys. Lett.* **2006**, *89*, 093504.

[68] L. Herlogsson, M. Cölle, S. Tierney, X. Crispin, M. Berggren, *Adv. Mater.* **2010**, *22*, 72.

[69] T. D. Anthopoulos, D. M. De Leeuw, E. Cantatore, P. Van't Hof, J. Alma, J. C. Hummelen, *J. Appl. Phys.* **2005**, *98*, 054503.

[70] T. D. Anthopoulos, B. Singh, N. Marjanovic, N. S. Sariciftci, A. Montaigne Ramil, H. Sitter, M. Colle, D. M. De Leeuw, *Appl. Phys. Lett.* **2006**, *89*, 213504.

[71] F. Ante, U. Zschieschang, R. T. Weitz, D. Kalblein, K. Kern, H. Klauk, "Low-voltage metal-gate top-contact organic thin-film transistors and complementary inverters with submicron channel length", presented at *Device Research Conference - Conference Digest, DRC*, **2009**.

[72] K.-J. Baeg, D. Khim, D.-Y. Kim, S.-W. Jung, J. B. Koo, I.-K. You, H. Yan, A. Facchetti, Y.-Y. Noh, *J. Polym. Sci., Part B: Polym. Phys* **2011**, *49*, 62.

[73] D. Bode, K. Myny, B. Verreet, B. van der Putten, P. Bakalov, S. Steudel, S. Smout, P. Vicca, J. Genoe, P. Heremans, *Appl. Phys. Lett.* **2010**, *96*, 3.

[74] B. K. Crone, A. Dodabalapur, R. Sarpeshkar, R. W. Filas, Y. Y. Lin, Z. Bao, J. H. O'Neill, W. Li, H. E. Katz, *J. Appl. Phys.* **2001**, *89*, 5125.

[75] M. Kitamura, Y. Kuzumoto, S. Aomori, Y. Arakawa, *Appl. Phys. Express* **2011**, *4*.

[76] H. Klauk, M. Halik, U. Zschieschang, F. Eder, D. Rohde, G. Schmid, C. Dehm, *IEEE Trans. Electron Devices* **2005**, *52*, 618.

[77] Y. Y. Lin, A. Dodabalapur, R. Sarpeshkar, Z. Bao, W. Li, K. Baldwin, V. R. Raju, H. E. Katz, *Appl. Phys. Lett.* **1999**, *74*, 2714.

[78] J. H. Na, M. Kitamura, Y. Arakawa, *Thin Solid Films* **2009**, *517*, 2079.

[79] B. Yoo, T. Jung, D. Basu, A. Dodabalapur, B. A. Jones, A. Facchetti, M. R. Wasielewski, T. J. Marks, *Appl. Phys. Lett.* **2006**, *88*, 082104.

[80] U. Zschieschang, F. Ante, M. Schlorholz, K. Kern, H. Klauk, "Deterministic and continuous control of the threshold voltage and noise margin of organic thin-film transistors and organic complementary circuits using mixed phosphonic acid self-assembled monolayer gate dielectrics", presented at *Device Research Conference, 2009. DRC 2009*, 22-24 June 2009, **2009**.

[81] R. A. Street, A. Salleo, *Appl. Phys. Lett.* **2002**, *81*, 2887.

[82] D. J. Gundlach, L. Zhou, J. A. Nichols, T. N. Jackson, P. V. Necliudov, M. S. Shur, *J. Appl. Phys.* **2006**, *100*, 024509.

[83] T. J. Richards, H. Sirringhaus, *J. Appl. Phys.* **2007**, *102*, 094510.

[84] L. Bürgi, T. J. Richards, R. H. Friend, H. Sirringhaus, *J. Appl. Phys.* **2003**, *94*, 6129.

[85] C.-A. Di, G. Yu, Y. Liu, X. Xu, Y. Song, Y. Wang, Y. Sun, D. Zhu, H. Liu, X. Liu, D. Wu, *Appl. Phys. Lett.* **2006**, *88*, 121907.

[86] J. Collet, O. Tharaud, A. Chapoton, D. Vuillaume, *Appl. Phys. Lett.* **2000**, *76*, 1941.

[87] J. Z. Wang, Z. H. Zheng, H. Sirringhaus, *Appl. Phys. Lett.* **2006**, *89*, 083513.

[88] K. Tsukagoshi, F. Fujimori, T. Minari, T. Miyadera, T. Hamano, Y. Aoyagi, *Appl. Phys. Lett.* **2007**, *91*, 113508.

[89] M. D. Austin, S. Y. Chou, *Appl. Phys. Lett.* **2002**, *81*, 4431.

[90] J. Liu, L. Herlogsson, A. Sawatdee, P. Favia, M. Sandberg, X. Crispin, I. Engquist, M. Berggren, *Appl. Phys. Lett.* **2010**, *97*, 103303.

[91] S. Scheinert, T. Doll, A. Scherer, G. Paasch, I. Horselmann, *Appl. Phys. Lett.* **2004**, *84*, 4427.

[92] N. Stutzmann, R. H. Friend, H. Sirringhaus, *Science* **2003**, *299*, 1881.

[93] M. Leufgen, A. Lebib, T. Muck, U. Bass, V. Wagner, T. Borzenko, G. Schmidt, J. Geurts, L. W. Molenkamp, *Appl. Phys. Lett.* **2004**, *84*, 1582.

[94] C. W. Sele, T. Von Werne, R. H. Friend, H. Sirringhaus, *Adv. Mater.* **2005**, *17*, 997.

[95] N. Zhao, M. Chiesa, H. Sirringhaus, Y. Li, Y. Wu, B. Ong, *J. Appl. Phys.* **2007**, *101*, 064513.

[96] L. Herlogsson, Y.-Y. Noh, N. Zhao, X. Crispin, H. Sirringhaus, M. Berggren, *Adv. Mater.* **2008**, *20*, 4708.

[97] J. N. Haddock, X. Zhang, S. Zheng, Q. Zhang, S. R. Marder, B. Kippelen, *Org. Electron.* **2006**, *7*, 45.

[98] A. Facchetti, M. H. Yoon, T. J. Marks, *Adv. Mater.* **2005**, *17*, 1705.

[99] J. Veres, S. D. Ogier, S. W. Leeming, D. C. Cupertino, S. M. Khaffaf, *Adv. Funct. Mater.* **2003**, *13*, 199.

[100] L.-L. Chua, J. Zaumseil, J.-F. Chang, E. C. W. Ou, P. K. H. Ho, H. Sirringhaus, R. H. Friend, *Nature* **2005**, *434*, 194.

[101] M.-H. Yoon, H. Yan, A. Facchetti, T. J. Marks, *J. Am. Chem. Soc.* **2005**, *127*, 10388.

[102] M. Zirkl, A. Haase, A. Fian, Sch, H. n, C. Sommer, G. Jakopic, G. Leising, nther, B. Stadlober, I. Graz, N. Gaar, Schw, R. diauer, S. Bauer-Gogonea, S. Bauer, *Adv. Mater.* **2007**, *19*, 2241.

[103] Y. Fujisaki, M. Mamada, D. Kumaki, S. Tokito, Y. Yamashita, *Jpn. J. Appl. Phys.* **2009**, *48*, 111504 (5 pp.).

[104] L. A. Majewski, R. Schroeder, M. Grell, *Adv. Funct. Mater.* **2005**, *15*, 1017.

[105] M. Halik, H. Klauk, U. Zschieschang, G. Schmid, C. Dehm, M. Schutz, S. Maisch, F. Effenberger, M. Brunnbauer, F. Stellacci, *Nature* **2004**, *431*, 963.

[106] J. M. Ball, P. H. Wobkenberg, F. B. Kooistra, J. C. Hummelen, D. M. de Leeuw, D. D. C. Bradley, T. D. Anthopoulos, *Synth. Met.* **2009**, *159*, 2368.

[107] S. Chao, M. S. Wrighton, *J. Am. Chem. Soc.* **1987**, *109*, 2197.

[108] S. Chao, M. S. Wrighton, *J. Am. Chem. Soc.* **1987**, *109*, 6627.

[109] M. Taniguchi, T. Kawai, *Appl. Phys. Lett.* **2004**, *85*, 3298.

[110] H. Shimotani, H. Asanuma, J. Takeya, Y. Iwasa, *Appl. Phys. Lett.* **2006**, *89*, 203501.

[111] J. Takeya, K. Yamada, K. Hara, K. Shigeto, K. Tsukagoshi, S. Ikehata, Y. Aoyagi, *Appl. Phys. Lett.* **2006**, *88*, 112102.

[112] M. J. Panzer, C. D. Frisbie, *J. Am. Chem. Soc.* **2005**, *127*, 6960.

[113] M. J. Panzer, C. R. Newman, C. D. Frisbie, *Appl. Phys. Lett.* **2005**, *86*, 103503.

[114] M. J. Panzer, C. D. Frisbie, *Adv. Funct. Mater.* **2006**, *16*, 1051.

[115] M. J. Panzer, C. D. Frisbie, *Appl. Phys. Lett.* **2006**, *88*, 203504.

[116] M. J. Panzer, C. D. Frisbie, *J. Am. Chem. Soc.* **2007**, *129*, 6599.

[117] A. S. Dhoot, J. D. Yuen, M. Heeney, I. McCulloch, D. Moses, A. J. Heeger, *Proc. Natl. Acad. Sci. U. S. A.* **2006**, *103*, 11834.

[118] J. D. Yuen, A. S. Dhoot, E. B. Namdas, N. E. Coates, M. Heeney, I. McCulloch, D. Moses, A. J. Heeger, *J. Am. Chem. Soc.* **2007**, *129*, 14367.

[119] E. Said, X. Crispin, L. Herlogsson, S. Elhag, N. D. Robinson, M. Berggren, *Appl. Phys. Lett.* **2006**, *89*, 143507.

[120] S. Ono, S. Seki, R. Hirahara, Y. Tominari, J. Takeya, *Appl. Phys. Lett.* **2008**, *92*, 103313.

[121] S. Ono, K. Miwa, S. Seki, J. Takeya, *Appl. Phys. Lett.* **2009**, *94*, 063301.

[122] T. Uemura, M. Yamagishi, S. Ono, J. Takeya, *Appl. Phys. Lett.* **2009**, *95*, 103301 (3 pp.).

[123] T. Uemura, M. Yamagishi, S. Ono, J. Takeya, *Japanese Journal of Applied Physics* **2010**, *49*, 01AB13 (3 pp.).

[124] T. Fujimoto, M. M. Matsushita, K. Awaga, *Chem. Phys. Lett.* **2009**, *483*, 81.

[125] J. Lee, M. J. Panzer, Y. He, T. P. Lodge, C. D. Frisbie, *J. Am. Chem. Soc.* **2007**, *129*, 4532.

[126] J. H. Cho, J. Lee, Y. Xia, B. Kim, Y. He, M. J. Renn, T. P. Lodge, C. D. Frisbie, *Nature Mater.* **2008**, *7*, 900.

[127] J. Lee, L. G. Kaake, J. H. Cho, X.-Y. Zhu, T. P. Lodge, C. D. Frisbie, *J. Phys. Chem. C* **2009**, *113*, 8972.

[128] Y. Xia, J. Cho, B. Paulsen, C. D. Frisbie, M. J. Renn, *Appl. Phys. Lett.* **2009**, *94*, 013304.

[129] D. Braga, M. Ha, W. Xie, C. D. Frisbie, *Appl. Phys. Lett.* **2010**, *97*, 193311.

[130] Y. Xia, W. Zhang, M. Ha, J. H. Cho, M. J. Renn, C. H. Kim, C. D. Frisbie, *Adv. Funct. Mater.* **2010**, *20*, 587.

[131] M. Hamedi, L. Herlogsson, X. Crispin, R. Morcilla, M. Berggren, O. Inganos, *Adv. Mater.* **2009**, *21*, 573.

[132] S. W. Lee, H. J. Lee, J. H. Choi, W. G. Koh, J. M. Myoung, J. H. Hur, J. J. Park, J. H. Cho, U. Jeong, *Nano Lett.* **2010**, *10*, 247.

[133] L. Kergoat, L. Herlogsson, D. Braga, B. Piro, M.-C. Pham, X. Crispin, M. Berggren, G. Horowitz, *Adv. Mater.* **2010**, *22*, 2565.

[134] L. Seung-Yong, C. Gyoung-Rin, L. Hyuneui, L. Kyung-Mi, L. Sang-Kwon, *Appl. Phys. Lett.* **2009**, *95*, 013113 (3 pp.).

[135] H. Shimotani, G. Diguet, Y. Iwasa, *Appl. Phys. Lett.* **2005**, *86*, 22104.

[136] K. H. Lee, S. Zhang, T. P. Lodge, C. D. Frisbie, *J. Phys. Chem. B* **2011**, *115*, 3315.

[137] P. Andersson, R. Forchheimer, P. Tehrani, M. Berggren, *Adv. Funct. Mater.* **2007**, *17*, 3074.

[138] P. Andersson, D. Nilsson, P. O. Svensson, M. Chen, A. Malmström, T. Remonen, T. Kugler, M. Berggren, *Adv. Mater.* **2002**, *14*, 1460.

[139] L. G. Kaake, Y. Zou, M. J. Panzer, C. D. Frisbie, X. Y. Zhu, *J. Am. Chem. Soc.* **2007**, *129*, 7824.

[140] T. Mills, L. G. Kaake, X. Y. Zhu, *Appl. Phys. A: Mater. Sci. Process.* **2009**, *95*, 291.

The Papers

Paper Overview

Paper I

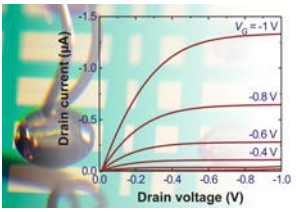

Low operating voltages for *p*-channel organic field-effect transistors (OFETs) can be achieved by using an electrolyte as the gate insulator. However, mobile anions in the electrolyte can lead to undesired electrochemistry in the channel. In order to avoid this, a polyanionic electrolyte is used as the gate insulator. The resulting OFET has operating voltages of less than 1 V (see figure) and shows fast switching (less than 0.3 ms) in ambient atmosphere.

Paper II

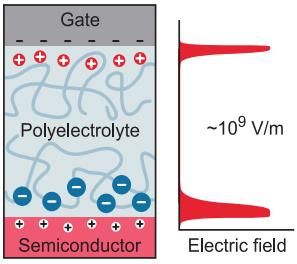

A polyelectrolyte is used as gate insulator material in organic field-effect transistors with self-aligned inkjet printed sub–micrometer channels. The small separation of the charges in the electric double layer at the electrolyte-semiconductor interface, which builds up in tens of microseconds, provides a very high transverse electric field in the channel that effectively suppresses short-channel effects at low applied gate voltages.

Paper III

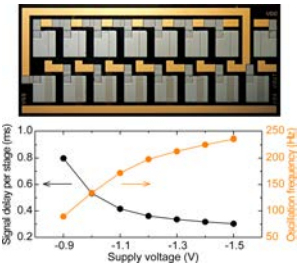

A polyanionic electrolyte is used as gate insulator in top-gate *p*-channel polymer thin-film transistors. The high capacitance of the polyelectrolyte film allows the transistors and integrated circuits to operate below 1.5 V. Seven-stage ring oscillators that operate at supply voltages down to 0.9 V and exhibit signal propagation delays as low as 300 μs per stage are reported.

Paper IV

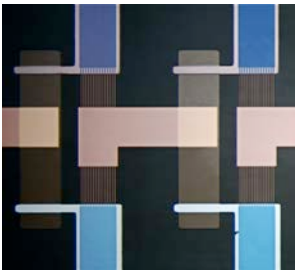

Organic complementary inverters and ring oscillators based on polyelectrolyte-gated thin-film transistors are demonstrated. Detrimental electrochemical doping is suppressed by using polyanionic and polycationic gate insulators in the *p*- and *n*-channel transistors, respectively. The circuits operate at supply voltages between 0.2 V and 1.5 V, have a static power consumption of less than 2.5 nW per logic gate and show propagation delays down to 0.26 ms per stage.

Paper V

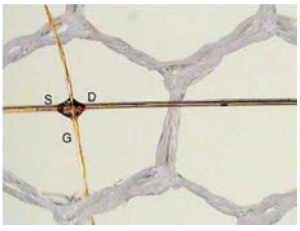

Electrolyte-gate organic field-effect transistors embedded at the junction of textile microfibers are demonstrated. The fiber transistor operates below 1 V, and delivers large current densities. The transience of the organic thin-film transistor's current and the impedance spectroscopy measurements reveal that the channel is formed in two steps.

Paper VI

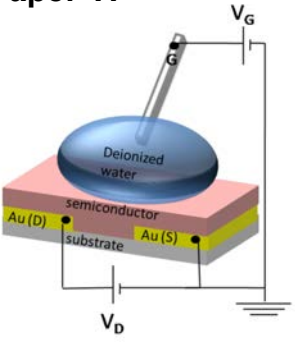

High-dielectric-constant insulators, organic monolayers, and electrolytes have been successfully used to generate organic field-effect transistors operating at low voltages. Here, we report on a device gated with pure water. By replacing the gate dielectric by a simple water droplet, we produce a transistor that entirely operates in the field-effect mode of operation at voltages lower than 1 V. This result creates opportunities for sensor applications using water-gated devices as transducing medium.